

Self-diffusion coefficient of bulk and confined water: a critical review of classical molecular simulation studies

Ioannis N. Tsimpanogiannis, Othonas A. Moulτος, Luís F. M. Franco, Marcelle B. de M. Spera, Máté Erdős & Ioannis G. Economou

To cite this article: Ioannis N. Tsimpanogiannis, Othonas A. Moulτος, Luís F. M. Franco, Marcelle B. de M. Spera, Máté Erdős & Ioannis G. Economou (2019) Self-diffusion coefficient of bulk and confined water: a critical review of classical molecular simulation studies, *Molecular Simulation*, 45:4-5, 425-453, DOI: [10.1080/08927022.2018.1511903](https://doi.org/10.1080/08927022.2018.1511903)

To link to this article: <https://doi.org/10.1080/08927022.2018.1511903>

 View supplementary material 

 Published online: 06 Sep 2018.

 Submit your article to this journal 

 Article views: 3576

 View related articles 

 View Crossmark data 

 Citing articles: 89 View citing articles 



Self-diffusion coefficient of bulk and confined water: a critical review of classical molecular simulation studies

Ioannis N. Tsimpanogiannis ^{a,b}, Othonas A. Moulτος ^c, Luís F. M. Franco ^d, Marcelle B. de M. Spera^d,
Máté Erdős^c and Ioannis G. Economou ^{b,e}

^aEnvironmental Research Laboratory, National Center for Scientific Research “Demokritos”, Aghia Paraskevi Attikis, Greece; ^bInstitute of Nanoscience and Nanotechnology, National Center for Scientific Research “Demokritos”, Aghia Paraskevi Attikis, Greece; ^cEngineering Thermodynamics, Process & Energy Department, Faculty of Mechanical, Maritime and Materials Engineering, Delft University of Technology, Delft, The Netherlands; ^dSchool of Chemical Engineering, University of Campinas, Campinas, Brazil; ^eChemical Engineering Program, Texas A&M University at Qatar, Doha, Qatar

ABSTRACT

We present a detailed overview of classical molecular simulation studies examining the self-diffusion coefficient of water. The self-diffusion coefficient is directly associated with the calculations of tracer or mutual diffusion coefficient of mixtures and, therefore, is a fundamental transport property, essential for an accurate description of mass transfer processes in biological, geological (i.e. energy or environmentally related), and chemical systems. In the current review we explore two distinct research areas. Namely, we discuss the self-diffusion of water in the bulk phase and under confinement. Different aspects that affect the diffusion process, including the molecular models, the system-size effects, the temperature and pressure conditions and the type of confinement are discussed. Finally, possible directions for future research are outlined.

ARTICLE HISTORY

Received 31 May 2018
Accepted 7 August 2018

KEYWORDS

Self-diffusion coefficient;
water; molecular simulations;
review

1. Introduction

Water is probably the most ubiquitous substance on earth and is directly involved in various aspects of biological processes in nature. It participates in the structure, stability, dynamics, and functions of proteins and other biomolecules [1]. It plays an important role in the development and sustainability of life and is also accounted in numerous aspects that are closely associated with everyday life (e.g. weather and atmospheric phenomena, the environment [2], industrial production [3], food science and technology). From a chemical point of view, water is a relatively non-complex substance that is composed by one oxygen and two hydrogen atoms. Yet, it is a highly associating dense fluid with long ranged interactions. Consequently, water has a very complex behaviour with the largest number of counterintuitive anomalies in its physical properties [4–6]. Currently, there are 73 anomalies listed (see for example [7]) and despite the immense research effort a number of them still remain unresolved. Numerous studies have appeared in the literature examining the various properties of interest of water.

Traditionally, these studies utilise an approach that typically can fall within one of the following four general groups of methods: (i) *ab initio*-based simulations, (ii) molecular simulations (e.g. molecular dynamics, MD and Monte Carlo, MC) based on empirical/semi-empirical force fields, (iii) effective continuum-scale theoretical methods, and (iv) experimental methods. Experiments are valuable tools for uncovering the fundamentals behind various phenomena. While experimental methods are also essential for testing the accuracy of computational methods, significant effort is also made to reduce the

amount of experimental work required for the confirmation of theoretical models or the validation of molecular-scale computational studies. Performing experimental measurements for all the possible water containing systems, at all possible state points, is rather impractical. To address the issue, two characteristic approaches can be followed. First, an effective-continuum theory can be developed and tested using the available experimental data. Such theoretical or semi-empirical models can be utilised for performing accurate and detailed studies at conditions within the range of development of the theoretical models. Nevertheless, care should be taken for applications at conditions outside the range of development of the models. A second, attractive alternative would be to use a limited amount of experimental measurements to design and validate appropriate interaction potentials (empirical/semi-empirical or *ab initio*), which can be subsequently used for extensive molecular-scale computational studies. This latter approach is gaining significant momentum as a result of the increase of available computational power and the development of more efficient computational methods [8–10].

Providing a detailed review of studies related to water would be a daunting task, even if we focused only at the relevant review papers. Consequently, the different review studies are topic-specific and traditionally focus on a limited amount of aspects related to water. The following studies are typical such reviews, among numerous reported in the literature: Debenedetti and Stillinger [11] discussed the complex interplay between dynamics and thermodynamics encountered in supercooled liquids, and particularly in water. Stanley et al. ([12–14])

discussed in detail the hypothesis of liquid polyamorphism, as a possible explanation for the anomalous behaviour of water. Bartels-Rausch et al. [15] reviewed the science behind ice structures and patterns. Wallqvist and Mountain [16] presented a detailed discussion on the derivation and description of molecular models for water. Vega and Abascal [4] proposed a quantitative test that can be used to evaluate the performance of various computational water force fields. The test was based on 17 properties of water considering the vapour, liquid and solid phases of water. Subsequently, the test was utilised to examine five rigid non-polarisable water force fields. Striolo et al. [17] discussed the challenges involved in the modelling of the carbon-water interface. Gillan et al. [18] presented a detailed discussion on the quality of the Density Functional Theory (DFT) for water.

The ACS journal *Chemical Reviews* dedicated recently an entire issue to water, entitled '*Water – The Most Anomalous Liquid*', where a number of topical reviews were presented. In the particular issue, Gallo et al. [6] provided a detailed review and explored several theoretical scenarios for the behaviour of water in the anomalous regime from ambient conditions all the way to the deeply supercooled region (i.e. 150–230 K at ambient pressure). Cisneros et al. [19] presented a review of the recent progress in the development of analytical potential energy functions that aim to represent correctly the many-body effects. Ceriotti et al. [20] presented the latest developments in the experimental, theoretical, and simulations studies of nuclear quantum effects in water. Fransson et al. [21] explored the use of X-ray and electron spectroscopy to probe water at different temperatures. Amann-Winkel et al. [22] discussed the use of X-ray and neutron scattering methods to study water structure at conditions ranging from ambient to deeply supercooled and amorphous states, while Perakis et al. [23] reported on the use of static and time-resolved vibrational spectroscopy of liquid water for the same conditions. Cerveny et al. [24] considered the study of water under geometrical confinement as a proxy of studying water in the deeply supercooled region (i.e. 150–230 K at ambient pressure). Such conditions are difficult to attain for bulk water since immediate crystallization to ice occurs.

The same pattern of approaching water is followed here as well. The current study focuses on the self-diffusion coefficient of water calculated with molecular simulations. Self-diffusion coefficient is a fundamental transport property that is essential for the accurate description of mass transfer processes and is involved in the design of various industrial separation processes [25]. Self-diffusion coefficient is also directly associated with the calculations of tracer or mutual diffusion coefficient of mixtures [26].

Furthermore, the self-diffusion coefficient is an important parameter because it is one of the few time-dependent properties that can be measured directly, using both experiments and simulations. Given that transport properties are intimately related to the short- and long ranged intermolecular potentials, the self-diffusion coefficient provides a fundamental test for a solvent model.

The objectives of the current study are the following: (i) to perform an exhaustive review of the available literature and collect the studies that report self-diffusion coefficient of water

obtained from molecular simulations (using empirical/semi-empirical force fields). An extended list of water-related studies, along with reported values and comments on the studies are provided in the Supporting Information. Emphasis is placed in two distinct research areas. The first considers studies of water in the bulk phase [27–197], while the second explores studies of water under confinement [198–286]. (ii) To present comparisons of the most reliable calculations with available experimental data [287–297]. (iii) To discuss issues that could affect the accuracy of the self-diffusion coefficient calculated using molecular simulations. Such issues include: the system size effects (SSE) [i.e. the common practice of using a few hundred molecules, leads to a significant deviation between the simulated (i.e. finite system size) and real (i.e. thermodynamic limit) self-diffusivity]; the use of rigid classical water force fields and the effect of polarizability on the self-diffusion coefficient; the effect of internal degrees of freedom; the effect of temperature and pressure including the supercooled and near- or supercritical regions; and the use of coarse-grained models.

Water under confinement is currently a very active research area. It is encountered in diverse environments such as in biological systems, industrial processes and geological settings associated with energy (e.g. oil and gas production, hydrate deposits in oceanic and permafrost regions) or environmental related applications (e.g. pollutant migration, carbon dioxide sequestration). Water under confinement has also been an alternative approach to study water at supercooled conditions, without the problem of ice formation. Confinement results in shifting the temperature where ice formation occurs to lower values [24].

Developing intermolecular potentials for simulations of liquids has been, so far, a compromise between computational efficiency and accuracy of the developed models [298]. Empirical or semi-empirical potentials, once they are developed, they are subsequently used extensively in common molecular simulation packages [8–10]. On the other hand, quantum chemical methods allow for the calculation of intermolecular forces during each time step of the simulation (a process known as 'on-the-fly' calculations). Such an approach is also known as the Car-Parrinello *ab initio* (CPAImD) MD simulation. Due to the significantly high computational cost, only small systems (16–128 molecules) have been studied over short periods. Water has been examined extensively (i.e. typical examples of such studies include refs. [299–334]) by such *ab initio* methods since the pioneering work of Laasonen et al. [299] who used 32 D₂O molecules for their simulations and reported a value for the self-diffusivity, $D_o = (2.2 \pm 1) \times 10^{-9} \text{ m}^2\text{s}^{-1}$, in good agreement with the experimental value. Note, however, that no system size effects were considered (see also the discussion in Section 2.1). The self-diffusivity is usually among the parameters examined in order to evaluate the performance of the *ab initio* models. However, in the current study we have focused primarily on self-diffusivities obtained from empirical/semi-empirical models and no systematic study was undertaken for the self-diffusivities obtained from *ab initio* models. Given the amount of studies available, this issue is probably worth a separate review.

Similarly, in this review paper we do not provide an in-depth discussion regarding the calculation of self-diffusivities using

reactive force fields in order to keep the number of references manageable for this study. Nevertheless, important advances in the use of reactive force fields for calculating transport properties of bulk and confined water have been reported during the recent years. Such is the case of the recent study by Manzano et al. [335] that found that ReaxFF [336] is able to simulate water properties in sub- and super-critical states in good quantitative agreement with experimental data. For further reading on this subject the reader is referred to ([337–340]) and references therein.

The manuscript is organised as follows: Initially, in Section 2 we present the related discussion of the self-diffusion coefficient of water in the bulk phase. Subsequently, in Section 3 we discuss the effect of confinement on the self-diffusion coefficient of water. We examine here the confinement in carbon compounds, minerals, biomolecules, and other materials. Finally, we end with future outlook and conclusions.

2. Bulk phase water self-diffusion coefficient

2.1. Finite size effects

As shown in a series of papers by Teleman and co-workers ([41,55,341,342]), the self-diffusion coefficient of water obtained from molecular simulations depends on the number of the molecules used (i.e. the system size) due to the long-range interactions and the imposed periodic boundary conditions. A systematic study on this subject was presented by Dünweg and Kremer [343], who performed MD simulations of a polymer chain in a good solvent and showed that hydrodynamic interactions in a finite system are expected to have strong effects on the dynamical properties of the system. The authors showed that solvent particle mobility scales linearly with $1/L$ (which is proportional to $1/N^{1/3}$), where L is the length of the simulation box (and N the number of molecules). Thus, $1/L = 0$ corresponds to the self-diffusivity at the thermodynamic limit, which is the quantity measured experimentally.

A decade later, Yeh and Hummer [102] performed a thorough study of Lennard-Jones (LJ) systems and TIP3P [32] water and observed that the same scaling behaviour applies also for the self-diffusion coefficient of small molecules (see Figure 2 of ref. [102]). Based on the work of Dünweg and Kremer, Yeh and Hummer presented an analytic term, based on the hydrodynamic theory for a spherical particle in a Stokes flow with periodic boundary conditions, which can be added to the MD computed self-diffusivity value in order to correct for the finite size dependences. Accordingly, the self-diffusivity of water at the thermodynamic limit, D_∞ , can be calculated from Equation (1):

$$D_\infty = D_{MD} + \frac{k_B T \xi}{6\pi\eta L} \quad (1)$$

where D_{MD} is the self-diffusivity obtained from MD simulations, k_B is the Boltzmann constant, T is the absolute temperature, ξ is a dimensionless constant which is approximately equal to 2.837297 for cubic simulation boxes, η is the shear viscosity of water and L is the length of the simulation box. As Equation (1) assumes, shear viscosity is independent of the system size ([102,343,344]). The second term of Equation (1)

is the analytic correction. It is important to note that since different water models yield different shear viscosity values, the shear viscosity for use in the correction should be also obtained from MD simulations. However, studies that used the experimental value in Equation (1) can be found in literature ([121,140,189]). Alternatively, if the viscosity is unknown, D_∞ can be obtained from the y intercept of the linear fit to two or more D_{MD} values, corresponding to different system sizes, as in the studies by Bauer and co-workers ([125,126]) and Troster et al. [172]. Very recently, Jamali et al. [345] showed that a similar correction to Equation (1) should be used for correcting the Maxwell-Stefan diffusion coefficient. Although, originally Equation (1) was derived by Dünweg and Kremer [343] and has been already mentioned in the work of Spångberg and Hermansson [99], Yeh and Hummer's study was, most probably, the first in which this term was actually applied to obtain the water self-diffusion coefficient at the thermodynamic limit.

Despite the fact that finite size dependences on the dynamic properties of water were already reported in the 80's, only a small fraction of the self-diffusivity values reported in the literature are corrected accordingly. This observation, combined with the fact that in most of the studies the number of water molecules used is rather low (below 1,000), makes the consistent evaluation of the numerous water force fields an arduous task. A characteristic example is the TIP4P/2005 [105], which is often characterised as the best condensed-phase water force field. The self-diffusivity at 298 K and 1 bar, reported in the original work by Abascal and Vega, was calculated from a system of 530 molecules (without correction) and was shown to underestimate the experimental value. However, after the appropriate correction, it ends up slightly (approx. by 1%) overestimating the experimental diffusivity. Similarly, the self-diffusion coefficient of TIP4P-Ew (Horn et al., [101]) at 298 K and 1 bar, in the original paper was calculated from a system of 512 molecules and shown to be $2.4 \times 10^{-9} \text{ m}^2/\text{s}$, which is only 4% higher than the experimental value ($2.3 \times 10^{-9} \text{ m}^2/\text{s}$ [289]). However, after the appropriate correction, the self-diffusivity value becomes $2.7 \times 10^{-9} \text{ m}^2/\text{s}$, which overshoots the experiment by 18%.

Due to the magnitude of the finite size dependences and the wide range of system sizes used in different studies (in the range of approx. 200–4,000 molecules), multiple values for the self-diffusivity of water are reported for each force field. In Figure 1, the self-diffusivity of water is shown as a function of the system sizes used in the MD simulations, for four of the most widely used force fields, namely the SPC [346], SPC/E [39], TIP4P [32], and TIP4P/2005 [105]. The values shown in Figure 1 are obtained from multiple sources. As it can be seen, for relatively high numbers of molecules (approx. 2,000) the distinction between the models is clear, with the exception of some outlying points. However, for the area of the plot showing the low numbers of molecules (i.e. below 500), the values calculated from different models overlap. Moreover, self-diffusivities obtained from small system sizes (approx. 100–300) are scattered, indicating that these calculations have much higher uncertainty. The latter is expected since self-diffusion coefficient is a single-molecule property (i.e. calculated from the mean square displacement (MSD) of every individual molecule

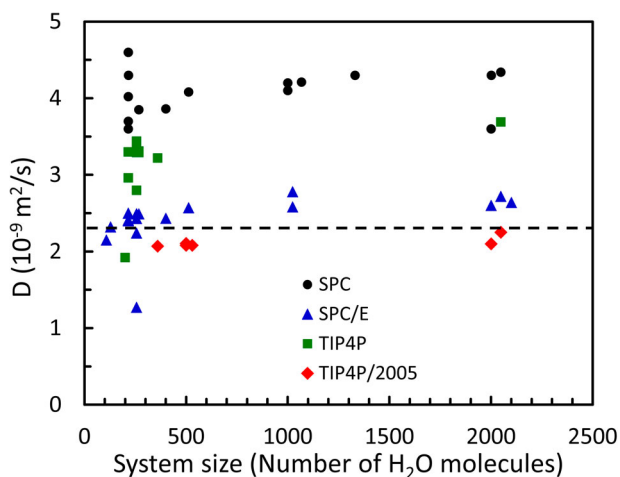


Figure 1. (Colour online) The diffusion coefficient of water at ambient conditions (i.e. 298/300 K and 1 bar) computed from widely used water force-fields as a function of the number of molecules used in the MD simulations. These values are not corrected for system size effects. The experimental data are collected from multiple studies: SPC ([39,43,56,57,83,95,99,108,137,139,148,150,170,173,177]); SPC/E ([39,43,44,61,62,83,90,99,108,121,139,148,156,157,169,173]); TIP4P ([36,40,43,83,91,121,123,139,157,161]); and TIP4P/2005 ([105,123,139,141,171,173]). The dashed line denotes the experimental value: $2.3 \times 10^{-9} \text{ m}^2/\text{s}$ [289].

in the system) and consequently the statistical uncertainty decreases by increasing the system size.

Attention also should be drawn to the fact that most of the studies do not report the exact methodology used to obtain the self-diffusivity and the respective statistical error. Pranami and Lamm [347] presented a rigorous approach for calculating accurate self-diffusion coefficient, highlighting the importance of running multiple independent and sufficiently long simulations as well as paying attention to the proper fitting to the mean squared displacement of the diffusing molecules. Wang et al. [348] and Casalegno et al. [349] have shown that long runs are needed in order for the molecules to get from the sub-diffusive regime into the (Gaussian) Fickian, from which accurate self-diffusivity values can be obtained in MD simulations. Although these studies focus on more viscous systems, the same principles apply to water and thus, particular attention should be paid in the actual displacement of the diffusing molecules, especially at low temperatures.

The self-diffusion coefficient, and transport properties in general, are not often taken into account in the parameterisation of water models, but calculated afterwards to validate their efficiency. However, if self-diffusivity is part of the parameterisation, it is crucial that the finite size effects are taken into account; otherwise the optimisation procedure will be inaccurate. This is the case for the polarisable SWM4 model ([107,350]), for which Lamoureux and co-workers took into consideration self-diffusion coefficient as a target property, but the value used was not corrected for finite size effects, resulting in a model that in reality significantly overestimates self-diffusivity (by approx. 20%). In the parameterisation procedure of the polarisable models SWM6 [158] and POL4D [144], the three-body potential E3B3 [183], and the SSMP [189] model, the self-diffusivity at ambient conditions was also used. In these four studies, the extrapolated self-diffusivity value was taken into account (by applying the correction of Equation (1)). However, in the case of SSMP the experimental

value for viscosity was used instead of the MD-computed one. This is expected to have an effect on the corrected value if the MD obtained viscosity deviates from the experimentally measured. Finally, Izaldi et al. [174] used self-diffusivity as a target property, in the fitting procedure of the OPC model, but the authors do not report if the system size used was the extrapolated to the thermodynamic limit.

Except from the finite system sizes, quantum nuclear effects are expected to have some effect in the MD calculations of the self-diffusion coefficient [77]. However, this effect according to Habershon et al. [351] is small and thus ignored in most of the studies.

2.2. Self-diffusion coefficient at ambient conditions

2.2.1. Rigid non-polarisable force fields

Since the pioneering work of Stillinger and co-workers ([27–30,352,353]) in the 1970s who presented the first ‘Computer Era Models’ [16], numerous models have been developed, trying to reproduce the most important thermodynamic and transport properties of water. The models by Matsuoka et al. [354], Jorgensen et al. ([32,355]) and Berendsen et al. ([39,346]) developed in the 1980s, formed the foundation for numerous others in the decades that followed. Already 30 years ago, the number of water force fields was such that Watanabe and Klein [43] stated: ‘... there are now probably more articles in the literature dealing with potential models for water than there are groups actually interested in using the potentials in molecular dynamics or Monte Carlo simulation studies ...’.

The majority of these water force fields are designed based on the concept of pairwise additivity. In that fashion, the total potential energy of the system can be expressed as the sum of pair interactions. This class of models implicitly incorporating the induced polarisation through optimised dipole moments and fixed point charges are called non-polarisable and are widely used due to their computational efficiency. Such interaction potentials are the well-known SPC-([39,108,346,356]) and TIP- ([32,101,105,357]) families.

The accurate prediction of the self-diffusion coefficient at ambient conditions (i.e. 298 K and 1 bar) is a highly desirable characteristic of any water model due to the potential use of the model as a predictive tool for relevant applications. To that end, one should expect that self-diffusivity is a common target property in force-field parameterisation. However, as already discussed previously (Section 2.1) this is not the case. In fact, only very few models are designed this way, while the prediction of self-diffusivity is very often based on the accurate prediction of other properties, e.g. liquid density and pair correlation function.

In this section, a brief discussion on the performance of various non-polarisable models will be presented, but given the huge amount of work done in this field and the inconsistency between some reported values, not all of the relevant studies will be analysed in order to keep this manuscript in a logical size. Additionally, it should be noted that although there exist more than a hundred different self-diffusion coefficient values reported in the literature for water at ambient conditions, only a small fraction of those are corrected for system size effects (see discussion in Section 2.1) and thus, an accurate

performance check of all water models in predicting self-diffusivity seems impossible to be achieved. Particularly, our search revealed that approximately 80% of the total available self-diffusivity values reported are computed from MD simulations of up to only 500 molecules. This directly leads us to the conclusion that the biggest part of the gathered data needs to be shifted upwards by 5–15%, to compensate for the finite size dependences. A collection of self-diffusion coefficient found in the open literature is gathered in Table SI–1 of the Supporting information, along with the original references. Detailed reviews on the various model types and their general performance can be found, in the works by Wallqvist and Mountain [16], Guillot [358] and Vega and Abascal [4].

In Figure 2, twelve different force fields are compared based on their ability to predict the self-diffusivity of water at ambient conditions. For the sake of a fair comparison, only results corrected for finite size effects are shown. The most accurate force field is found to be the E3B ([121,140]), which achieves ‘perfect’ agreement with the experimental self-diffusion coefficient ($2.3 \times 10^{-9} \text{ m}^2/\text{s}$ [289]). E3B model adopts the gas phase geometry of water and considers explicit three-body interactions, which were obtained from electronic structure calculations. The model is one of the few exceptions in which self-diffusivity at ambient conditions was used in the fitting procedure (corrected for system size effects according to Equation (1), but with the experimental viscosity value). As can be seen from Figure 2, later versions of the E3B model, namely the E3B2 [359] and E3B3 [183], are also relatively accurate. At this point one should argue that a comparison of two-body potentials (i.e. all models in Figure 2 except from the E3B family) with the E3B family is unfair, exactly because the latter ones include three-body short ranged interactions. However, the incorporation of these additional interactions does not necessarily lead to better self-diffusivity predictions. Characteristic is

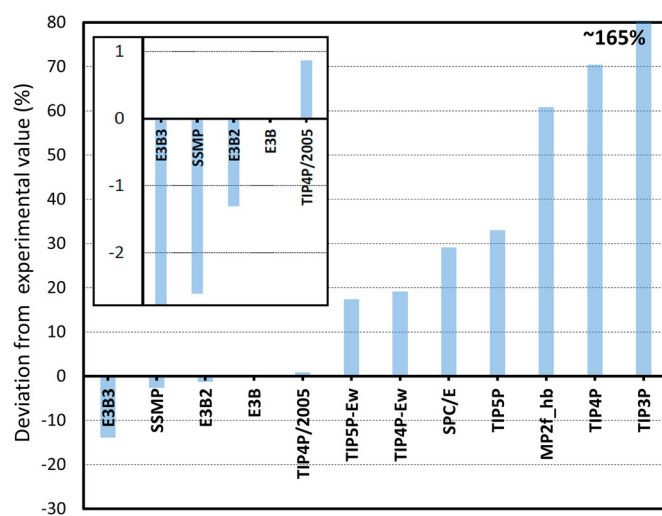


Figure 2. (Colour online) The relative deviation of self-diffusion coefficient from the experimental value at ambient conditions ($2.3 \times 10^{-9} \text{ m}^2/\text{s}$ [289]), obtained by various force fields. MD obtained values are corrected for finite size effects (see Section 2.1). The actual values of the self-diffusivities can be found in Table SI–1 of the Supporting Information. The experimental data are collected from multiple studies: E3B3 [183]; SSMP [189]; E3B2 [183]; E3B [140]; TIP4P/2005 [183]; TIP4P-Ew [159]; TIP5P-Ew [159]; SPC/E [152]; TIP5P [159]; MP2f_hb [129]; TIP4P [159]; TIP3P [149].

the case of the three-body potential version of the MCY model [37], the diffusion and reorientation dynamics of which are much slower, compared to the original two-body MCY ([31,354]) and the experimental value. For a general discussion on the effect of three-body interactions in water simulations the reader is referred to the work by Wojcik and Clementi [37].

TIP4P/2005 [105] self-diffusivity predictions are shown to be very accurate, deviating less than 1% from the experimental value, making it by far the best performing among the TIP family. As Vega and Abascal [4] observed, models like TIP4P/2005 that overestimate the vaporisation enthalpy of water by 10–15% tend to give quite reliable self-diffusion coefficient. In the same manner, models fitted to reproduce the vaporisation enthalpies like TIP3P [32], TIP4P [360] and TIP5P [357] tend to significantly overestimate the self-diffusivity value (deviation of more than 30% from the experimental value). More particularly, TIP3P has the lowest predictive ability for the self-diffusion coefficient of water, deviating from the experimental value by almost a factor of 2. This failure can be partially attributed to the inability of TIP3P to properly reproduce the water structure. That was the reason which led to the design of TIP4P, in which the introduction of a dummy site carrying the negative charge instead of the oxygen atom improved both the prediction of water structure and the self-diffusion coefficient. As it can be seen in Figure 2, is much closer to the experimental value compared to the TIP3P and TIP4P. TIP5P features positive charges placed on the hydrogen sites and two negative ones in the so called ‘lone pair electrons’ positions, in an attempt to describe the water molecule in a more chemistry-accurate way.

In 2004, Rick [361] and Horn et al. [101] presented the TIP5P-Ew and TIP4P-Ew models, which are re-optimised versions of the TIP5P and TIP4P, respectively. In these models the long-ranged electrostatic interactions are treated with Ewald techniques, instead of simple spherical cut-offs. Both models give much improved self-diffusivity predictions (below 20% deviation from the experimental value), as shown by Yu et al. [159], who presented a series of self-diffusion coefficient calculations by taking into consideration the system size dependences.

2.2.2. The effect of polarizability

As discussed previously, most water models up to date are pairwise additive and treat electrostatic interactions through fixed point charges. However, many important forces are of non-additive nature, with the most important of those being the electronic polarizability. Polarizability is the quantity measuring the relative tendency of the electron cloud of a molecule to be distorted from its normal arrangement in the presence of an electric field. In a homogeneous condensed system, like bulk water, the effect of polarisation is almost isotropic. With this in mind, and given that liquid is the most common form of water in nature, the main targets of research groups developing force fields are usually bulk water properties (e.g. density, internal energy, dielectric constant, structural, and perhaps transport properties). Although non-polarisable force fields may perform reasonably well for liquid water at ambient conditions (see Figure 2), in which the instantaneous environment of each molecule is very similar

to the average environment, it is expected that they are less accurate for inhomogeneous systems (e.g. close to surfaces, near ions or biomolecules, multiple phases in the same simulation, binary and multicomponent mixtures) or for predicting properties spanning the entire phase diagram. To overcome these inherent limitations, force fields that include a many-body polarizability term have been developed. These models are called polarisable, and based on the approach to treat polarisation, can be divided in four groups, namely models with (a) induced molecular point dipoles or multipoles, (b) induced atomic dipoles, (c) classical Drude oscillators (or Shell model), and (d) fluctuating charges. For thorough discussions on polarisable models the reader is referred to the studies by Wallqvist and co-workers ([16,42]), Soetens and Millot [66], Fanourgakis and Xantheas [110], Kolafa [118], Lopes et al. [362], Kiss and Baranyai [160], Yu et al. [159], Tröster et al. [166], and Jiang et al. [190].

As already mentioned, self-diffusivity is very rarely taken into account as a target property in the parameterisation of a water model. In contrast, being a very important transport property, it is often computed to assess the predictive ability of the force fields. Thus, a logical question is: ‘how much and in what way the explicit description of water polarisation affects the self-diffusion coefficient predictions at ambient conditions?’ As already discussed, for bulk water the effect of polarisation is nearly isotropic and therefore, an average effective potential is expected to give quite satisfactory results. However, multiple polarisable force fields have been utilised for predicting the self-diffusivity of bulk water. In Figure 3(a), the deviation from experimental data of self-diffusion coefficient computed from various polarisable force fields is shown. Although, more results do exist in the literature (for the same or other models), we show only the values that are reported to be corrected for finite size effects, either by using Equation (1) or by fitting to multiple system sizes and extrapolating to the thermodynamic limit (see Section 2.1). Most of the models give rather satisfactory predictions (deviation approx. 15%), with the TIP4P-QDP-LJ [126] and TL6P [172] force fields being 100% accurate (0% deviation from the experimental value). This finding is quite interesting since self-diffusivity was not considered as a fitting parameter in the original development of these two models. TIP4P-QDP-LJ model is a modified version of TIP4P-QDP [125], which incorporates polarizability dependence in the repulsion and dispersion LJ terms. TIP4P-QDP-LJ model is able to predict density, self-diffusivity, enthalpy of vaporisation, dielectric constant, and the liquid–vapour coexistence curve quite accurately. TL6P is a six-point model (belonging to the TLvP [166] family), which is developed by applying DFT/PMM hybrid techniques [363], and except for the excellent prediction of the diffusion coefficient, it is also able to reproduce very accurately a series of liquid-phase properties of water, including the temperature of the maximum density, T^{md} . Recent models like the BK3 [160] and HBP [190] are also in good agreement with the experimental diffusivity value (deviation approx. 1% and approx. 5%, respectively). These two models utilise Drude oscillators with Gaussian charges, to model polarizability, and the Buckingham potential for the dispersion interactions. In the case of HBP, a short-ranged directional hydrogen-bonding

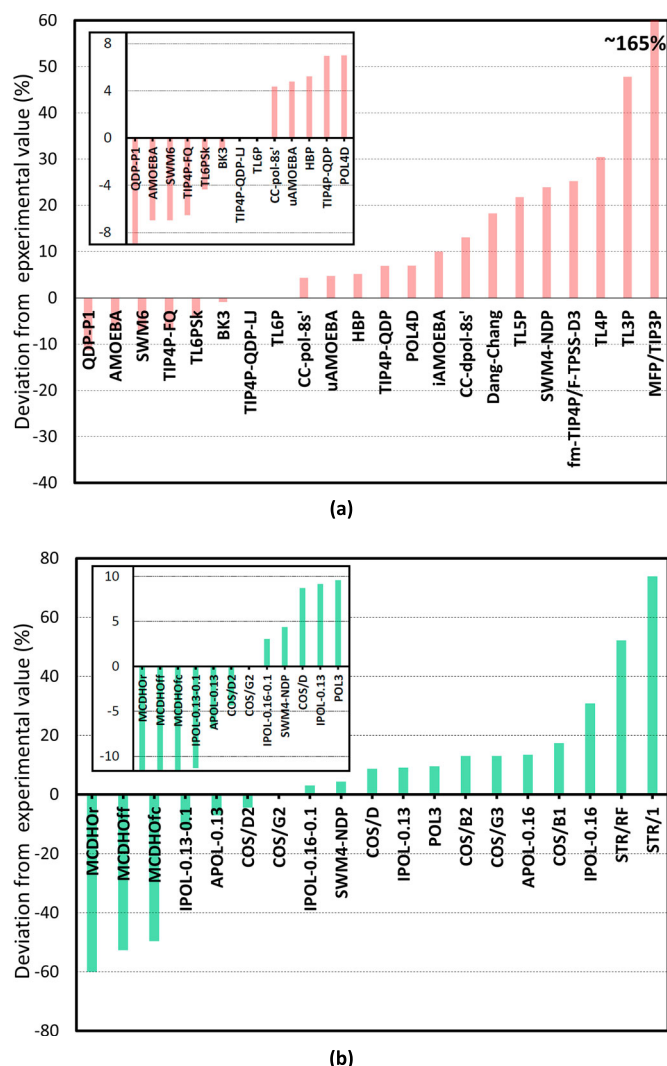


Figure 3. (Colour online) The relative deviation of self-diffusion coefficient from the experimental value at ambient conditions ($2.3 \times 10^{-9} \text{ m}^2/\text{s}$ [289]), obtained by various polarisable force fields. (a) MD-obtained values are corrected for finite size effects (see Section 2.1), (b) MD simulations of 1,000 molecules or more without corrections for finite size effects. The actual values of the self-diffusivities can be found in Table SI-1 of the Supporting Information. *For AMOEBa we used the value reported by Yu et al. [159]. Wang et al. [167] reports D for AMOEBa to be equal to $2.0 \times 10^{-9} \text{ m}^2/\text{s}$ which has a relative deviation from the experimental value equal to -13% . The experimental data are collected from multiple studies: (a): QDP-P1 [125]; AMOEBa [159]; SWM6 [159]; TIP4P-QDP [125]; TL6P^{sk} [172]; BK3 [160]; TIP4P-QDP-LJ [126]; TL6P [172]; CC-pol-8s' [158]; uAMOEBa [364]; HBP [190]; TIP4P-QDP [125]; POL4D [159]; iAMOEBa [167]; CC-dpol-8s' [158]; Dang-Chang [152]; TL5P [166]; SWM4-NDP [159]; fm-TIP4P/F-TPSS-D3 [175]; TL4P [166]; TL3P [166]; MFP/TIP3P [149]. (b): MCDHO_r [104]; MCDHO_{ff} [104]; MCDHO_{fc} [104]; IPOL-0.13-0.1 [118]; APOL-0.13 [118]; COS/D2 [170]; COS/G2 [365]; IPOL-0.16-0.1 [118]; SWM4-NDP [165]; COS/D [128]; IPOL-0.13 [118]; POL3 [118]; COS/B2 [95]; COS/G3 [365]; APOL-0.16 [118]; COS/B1 [95]; IPOL-0.16 [118]; STR/RF [95]; STR/1 [95].

interaction term is part of the potential and therefore water structure is also captured accurately.

Particularly interesting is the case of the SWM6 model. Although it was originally parameterised with self-diffusion coefficient as one of the target properties, its prediction deviates approx. 7% from the experimental value. Another, interesting case is the MFP/TIP3P model by Leontyev and Stuchebrukhov [149], which performs equally poorly with TIP3P (deviation from experiment approx. 165%), regardless of the inclusion of polarisation. These two examples show that by taking the

electronic polarizability of water into account when designing a model is insufficient to guarantee an accurate prediction of the self-diffusion coefficient.

As shown in Figures 3(a,b), relatively accurate values of self-diffusivity at ambient conditions can be obtained by various other polarisable models, belonging to diverse families and types. Some of those are the CC-pol-8s' [158], uAMOEBA [364] and TL6P^{sk} [172]. Although the diffusivity predictions of the models presented in Figure 3(b) are not corrected for finite size effects, the use of at least 1,000 molecules is expected to yield a relatively good prediction (possibly within 10–15%, depending on the accuracy in the computed viscosity) and therefore some force fields of the IPOL- and COS/- families are expected to be close to the experimental value. For more information on these models, the reader is referred to the original papers ([118,170,365]). Other polarisable water force fields, not presented here (see Table SI-1 in the Supporting Information), which exhibit relatively good self-diffusion coefficient predictions are: (a) the TTM2-R [89], which employs Thole-Type polarisable dipoles, (b) the Gaussian charge GCPM (Paricaud et al., [366]), which yields accurate predictions of various water properties for a wide range of conditions, and (c) the HBB2-pol [151], a full-dimensional model based on first principles.

The total average deviation between experimental data and calculations from the models listed in Figure 3(a) is approx. 19%, while the corresponding total average deviation of non-polarisable models shown in Figure 2 is 34%. This difference, although is not by any means a rigorous physical comparison, indicates that on average models with explicit polarisation do provide improved self-diffusivity predictions. Such differences are expected to be much more pronounced when surface phenomena or ionic systems are examined ([367,368]). As the results presented in Figure 3 suggest, the vast majority of the polarisable water force fields tend to overestimate self-diffusion coefficient. This finding could be attributed to several facts. For instance, although density predictions are in most of the cases quite accurate, the degree of hydrogen bonding between water molecules may not be correctly captured. In addition, the actual intermolecular energy plays a significant role, as the attractive and repulsive interactions can affect vastly the dynamic behaviour of the liquid. Finally, the dipole moment of the water molecule in each force field hugely affects the dynamic behaviour, since it affects the actual intermolecular interactions.

From the computational point of view, although comparisons between models are difficult to make, due to the plethora of different characteristics (e.g. number of sites, treatment of polarisation etc.), polarisable models, such as the ones presented above, are expected to require more computer time compared to the non-polarisable ones, with the same number of atomic sites. More specifically, as shown by Jiang et al. [369] the SWM4-NDP [107] model implemented in NAMD simulation package [370] has shown an increase in computational cost by approximately a factor of 2 compared to the TIP3P force field [32]. Similarly, the HBP polarisable force field by Jiang and co-workers [190] is 3 times slower compared to the nonpolarizable TIP4P/2005 [105]. Therefore, the additional computational demand justifies up to a point, the dominant use of non-polarisable models by the molecular simulation community.

2.2.3. The effect of internal degrees of freedom

The most widely-used water models assume that the intra-molecular degrees of freedom are frozen and thus treat the water molecule as a rigid object. To that end, the geometric characteristics of water models are usually based on experimental findings for an isolated molecule in the gas phase. The arguments for employing such a simplified model are both technical and physical (Berendsen et al. [346], Anderson et al. [38]). From the technical point of view, the computational time needed for simulating a system containing fully flexible molecules is higher, due to the introduction of bonded interactions and the lower simulation time-step needed (up to 5 times lower [141]) for the proper integration of Newton's equation. Although, this was a great issue in the early days of molecular simulations, nowadays with the huge increase in computational power and the availability of highly parallelizable open-source codes (LAMMPS [9], GROMACS [10], and NAMD [370]), such effects can be mitigated up to a point, especially for simulations of bulk fluids. A physical argument against the use of flexible models is that the internal vibrations in a water molecule are of quantum nature and thus cannot be properly modelled with classical mechanical approximations (Tironi et al. [371]). In addition, one can argue that at standard conditions $\hbar \omega_i \gg k_B T$ (where \hbar is the Planck constant, and ω_i is the angular frequency of the i th normal mode of vibration) and therefore the intra-molecular degrees of freedom are negligible [372].

On the other hand, arguments for employing a flexible water model are also common in literature. Lemberg and Stillinger [372] in 1975 presented the central force (CF) model for water, which includes intra-molecular degrees of freedom. This choice was based on the idea that even at low to moderate temperatures, the influence of zero-point motions and the possibility of static distortions due to the nature of hydrogen bonds still exist and should be reckoned with. Based on the CF model, the BJH [373] and RWK [374] water force fields modified the intra-molecular potential in a try to better capture the dynamics of the condensed phase. Lie and Clementi [35] extended the MCY model [354] to include intra-molecular vibrations, based on the idea that those motions in liquid water differ from the respective of an isolated water molecule, which are implicitly averaged and used in the rigid geometry. An interesting analysis on the effect of flexibility in the structural and dynamic properties of water for CF-type potentials is provided by Smith and Haymet [56]. Moreover, molecular simulations of flexible water make possible the investigation of properties related to its infrared and Raman spectra, and their relation with the hydrogen bonding network ([375,376]).

Based on the context discussed above a reasonable question is: '... how flexibility affects the prediction of self-diffusion coefficient?'. Teleman and co-workers ([41,55]) worked towards answering this question by performing MD simulations of the original rigid (Berendsen et al. [346]) and a flexible version of SPC model (Anderson et al. [38]). In their first article [41] they concluded that the introduction of flexibility in the SPC model vastly affects the kinetic behaviour of the system resulting in approximately 40% higher self-diffusivity. However, in their second article [55], in which both a harmonic and an anharmonic potential was used to describe the intra-molecular vibrations, self-diffusivity was shown to be

slower by 15–26%. The reason for this behaviour was that the flexible model exhibited an increased dipole moment, which causes the strengthening of the cohesive forces in the fluid. The increased dipole moment is in fact a polarisation response to the local electric field for the water molecule. The discrepancy between these two studies of Teleman and co-workers was attributed to the insufficient equilibration and the thermostat used in the simulations of the first paper [41].

Similar conclusions for various flexible realizations of the SPC model ([38,108,356,377]), were also drawn by the studies of Barrat and McDonnald [49], Lobaugh and Voth [77], English and MacElroy [91], Amira et al. [100], and Wu et al. [108]. The findings of these studies suggest that the self-diffusion coefficient decreases significantly when vibrational degrees of freedom are introduced to the SPC model, due to the increased dipole moment and radius of gyration of the flexible molecule. Wu et al. [108] specifically pointed out that the equilibrium bond length is a key factor affecting self-diffusivity, mainly due to its effect on the strength of the hydrogen bonds. Thus, the predictions from the flexible SPC models were shown to be closer to the experimental self-diffusivity value.

Other types of flexible models include the F3C by Levitt and co-workers [76], a force field specifically designed for simulations with macromolecules, and the TIP4P/2005f by Gonzalez and Abascal [141], which is the flexible version of the popular TIP4P/2005. According to the original papers, the self-diffusion coefficient of F3C is very close to the experimental value (deviation of approx. 4%), while TIP4P/2005f is less accurate compared to its rigid predecessor, underestimating the experimental value by approx. 16%.

At this point it is important to note that for none of the already discussed flexible water models the finite size dependency of the self-diffusion coefficient were taken into account, and thus the exact comparisons with the experimental values cannot be quantitatively accurate. In most of the above cases, a significant correction is needed due to the fact that the number of molecules used in the simulations was in the range of 100–300 molecules. In fact, the only corrected self-diffusion coefficient available in literature for flexible water models are given by Yu et al. [159], Wang et al. [167] and Spura et al. [175], for the polarisable force fields AMOEBA ([98,103]), iAMOEBA [167] and fm-TIP4P/F-TPSS-D3 [175]. The values are shown in Figure 3(a) and Table SI-1 of the Supporting Information.

The idea of further improving the structural, thermodynamic and kinetic property predictions of water by incorporating both flexibility and polarizability led to the design of many flexible polarisable force fields ([53,60,78,85,86,96,98,103,110,111,119,124,142,151,167,175,378–381]). The values for the reported self-diffusion coefficient from this type of force fields are gathered in Table SI-1 of the Supporting Information. In summary, some flexible polarisable models that provide quite accurate self-diffusivity values are the AMOEBA ([98,103]), MB-pol ([381,382]), PFG [96], HBB2-pol [151], and POLIR [119]. As mentioned above, a purely quantitative analysis of the self-diffusivity predictions of these models is impossible due to divergence in the system size used in each study. However, the effect of grafting flexibility onto a rigid polarisable force field is the same as with the non-polarisable

models. For instance, Jeon et al. [96] presented the Polarflex, a three-site flexible polarisable model for water, and compared it with its rigid version. Consistently to the studies of non-polarisable models, the self-diffusion coefficient was found to be lower for the flexible force field. Similarly, Fanourgakis and Xantheas [110] showed that the flexible version of their polarisable Thole-type model, known as TTM2.1F, was diffusing much slower (approx. 30%) compared to the rigid TTM-R [89].

2.2.4. Self-diffusion coefficient from coarse-grained models

Coarse-grained models have been widely employed in MD simulations to increase the accessible system size and time scales by using single particles (commonly called beads) to represent groups of nearby atoms. Nevertheless, this rough resolution of the smoothed potential energy surface can be a problem when dealing with small molecules such as water (Fuhrmans et al., [137]). Many models have been developed aiming at finding a balance between accurate representation of water properties and reasonable computational effort.

Fuhrmans et al. [137] modified SPC water model by introducing bundling through a restraining potential with tetrahedral shape geometry (four water molecules per bead). The higher hydrodynamic radius should give lower diffusion coefficient due to larger friction. However, the authors considered the SPC values for self-diffusion as four independent bundled water molecules, which gave similar but higher values (Table 1). This is believed to be likely due to coordinated movement enforced by the bundling.

Karamertzanis et al. [135] developed an anisotropic rigid-body potential to model the properties of water and the hydration free energies of neutral organic solutes. Their multipole model includes average polarisation effects of clusters of 225–250 water molecules and fits repulsion-dispersion parameters to liquid water experimental data. Although some properties like density are very close to the experimental value, self-diffusion was significantly underestimated (i.e. $1.4 \times 10^{-9} \text{ m}^2/\text{s}$ while the experimental value is $2.3 \times 10^{-9} \text{ m}^2/\text{s}$ at 298 K [289]).

Darre et al. [136] presented the WT4 potential, in which four interconnected beads in a tetrahedral conformation carry an explicit partial charge. Each cluster represents the movement of approximately eleven water molecules. The values of the self-diffusion coefficient obtained at different temperatures are in good agreement with experimental values.

A coarse-grained model based on Morse potential form (named CSJ) was described by Chiu et al. [134] with four water molecules per bead. The self-diffusion coefficient at

Table 1. Diffusion coefficient values for SPC modified 4-water bead by Fuhrmans et al. [137].

Model	D ($10^{-9} \text{ m}^2/\text{s}$) at 298 K	D ($10^{-9} \text{ m}^2/\text{s}$) at 323 K
Model 1 ^a	1.26 ± 0.05	1.80 ± 0.11
Model 2 ^a	1.24 ± 0.07	1.81 ± 0.10
SPC	1.05	1.55

^aThe models differ by the force constant of the restraining potential and the C_{12} LJ parameter. Model 1 has a lower force constant and allows greater deformation of the water clusters. Model 2 has a fourfold higher force constant that keeps the tetrahedral conformation constant and avoids overlaps in the coarse-grained representation.

298 K is overestimated ($4.3 \times 10^{-9} \text{ m}^2/\text{s}$) when compared to the experimental value.

The ELBA force field, a new parameterisation of the Stockmayer potential introduced by Orsi and Essex [145], is an electrostatic based potential in which each water molecule is represented by a soft LJ sphere embedded with a point dipole. LJ and inertial parameters were tuned to capture the experimental data for the bulk density and the self-diffusion coefficient. As a result, the dynamic behaviour of water is in good agreement with experimental and molecular-scale models at 298 K and 1 bar, as clearly shown in Table 2. Table 2 shows a comparative assessment between coarse-grained models, as obtained from Orsi [176]. The ELBA force field was also used to evaluate properties of water confined within mesoporous material and representative results for diffusion coefficient behaviour along the pore radius have been reported (Yamashita and Daiguji, [268]).

2.3. The effect of temperature and pressure on self-diffusion coefficient

2.3.1. The effect of temperature on self-diffusion coefficient at ambient pressure

Extensive MD simulations in the range of 220–370 K at 1 bar have been reported in the literature (see also Table SI–2 in the Supporting Information). It should be noted, however, that only a limited number of studies have included system size corrections in the MD-calculated water self-diffusion coefficient. Such cases are the following: Wang et al. [167] reported values for iAMOEBa [167] and AMOEBa [103]; Kiss and Baranyai [179] used BK3 [160]; Tran et al. [189] used SSMP that was introduced in the same study; Qvist et al. [147] used SPC/E [39]; and Guillaud et al. [194] used TIP4P/2005f [141].

SPC/E is a rigid classical water force field; TIP4P/2005f is a flexible version of the classical rigid TIP4P/2005 water force field, while the remaining four are polarisable interaction potentials. An extensive discussion of such types of force field has been also presented earlier in Sections 2.2.1–2.2.3. Figure 4 shows a plot of the water self-diffusion coefficient as a function of temperature at 1 bar, considering only those studies that have reported corrections accounting for system size effects. We observe that an increase in temperature results in an

Table 2. Self-diffusion coefficient of water for different coarse-grained models at 298/300 K.

Model	D ($10^{-9} \text{ m}^2/\text{s}$)	Water molecules \rightarrow interaction sites
ELBA ^a	2.16	1 \rightarrow 1
SSD ^a	1.78–2.51	1 \rightarrow 1
SSDQO ^a	2.21–2.26	1 \rightarrow 1
M3B ^a	1.7	1 \rightarrow 1
mW ^a	6.5	1 \rightarrow 1
MARTINI ^a	2.0	4 \rightarrow 1
P-MARTINI ^a	2.5	4 \rightarrow 3
GROMOS ^a	6.9	5 \rightarrow 2
WT4 ^a	2.23	11 \rightarrow 4
Mie (8-6) CGW1-vle [184]	1.7	1 \rightarrow 1
Mie (8-6) CGW1-ift [184]	7.4	1 \rightarrow 1
Mie (8-6) CGW2-bio [184]	3.8	2 \rightarrow 1
Experimental [289]	2.3	–

^aReferences of studies reporting self-diffusivities can be found in Orsi [176].

increase of the self-diffusion coefficient of liquid water. The temperature dependence of the MD-calculated self-diffusion coefficient of water can be accurately described using either a Speedy–Angel power-law [383] or a Vogel–Fulcher–Tamann (VFT) equation [383]. Additional discussion on this issue will be provided in Section 2.3.3.

In Figure 4 the MD-calculated values for the self-diffusion coefficient of water are also compared with experimental data obtained from a Speedy–Angel-type correlation reported by Qvist et al. [147]. The authors reported that in the temperature range 253–293 K the experimental self-diffusion coefficient, obtained from NMR pulsed gradient spin echo [384] or tracer measurements [287], can be represented by the following power-law expression:

$$D_{NMR}/10^{-10} \text{ m}^2 \text{ s}^{-1} = 159 \left(\frac{T/\text{K}}{212.6} - 1 \right)^{2.125} \quad (2)$$

Similarly Holtz et al. [385] reported that the available experimental data, in the temperature range 273–373 K, can be optimally fitted (i.e. with an error limit of $\leq 1\%$) with a Speedy–Angel power-law that has the following form:

$$D = D_o \left(\frac{T}{T_s} - 1 \right)^\gamma \quad (3)$$

where $D_o = (1.635 \times 10^{-8} \pm 2.242 \times 10^{-11}) \text{ m}^2 \text{ s}^{-1}$, $T_s = (215.05 \pm 1.20) \text{ K}$ and $\gamma = (2.063 \pm 0.051)$. As can be observed in Figure 4, at 1 bar all the water force fields considered, give accurate self-diffusion coefficient, with the least accurate being AMOEBa (underestimation) and SPC/E (overestimation).

Based on the discussion presented in Sections 2.1 and 2.2, we also examine the self-diffusion coefficient of water for those studies that lack corrections for system size effects, however, used 1,000 or more water molecules in the study. Figure 5(a) shows a plot of the water self-diffusion coefficient as a function

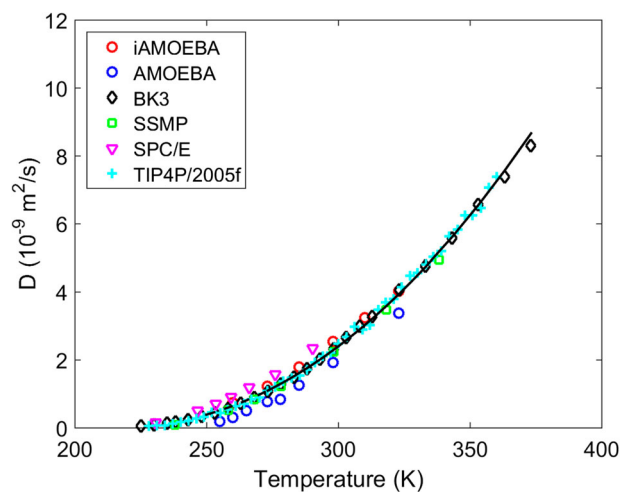


Figure 4. (Colour online) Water self-diffusion coefficient as a function of temperature at 1 bar. Symbols denote MD studies that have included system size corrections in the calculations: iAMOEBa [167]; AMOEBa [167]; BK3 [179]; SSMP [189]; SPC/E [147]; and TIP4P/2005f [194]. The black lines denote Speedy–Angel-type correlations of experimental data (solid line: experimental data of Holtz et al. [385] in the temperature range 273–373 K; dashed line: experimental data of Qvist et al. [147] in the temperature range 253–293 K).

of temperature at 1 bar, considering studies ([139,173,365]) that used rigid non-polarisable water force fields, while in Figure 5(b) all remaining available studies ([165,192,365]), using polarisable and *ab initio* models, are collected. Among the rigid non-polarisable water force fields that are included in Figure 5(a) are SPC [346], SPC/E [39], TIP4P [32], TIP4P-Huang [386], and TIP4P/2005 [105]. It can be seen in Figure 5(a) that the earlier versions of the SPC- and TIP4P-type water force fields significantly over-predict the self-diffusion coefficient of water at 1 bar. The TIP4P-Huang (Huang et al. [386]) is a TIP4P-type empirical model, optimised to reproduce

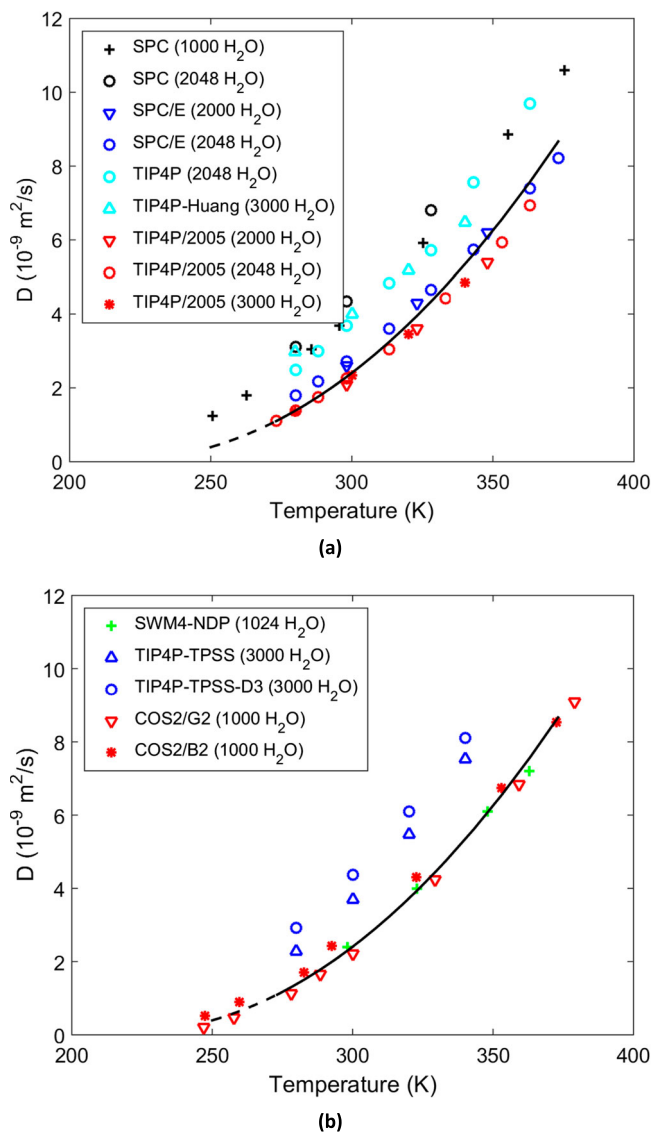


Figure 5. (Colour online) Water self-diffusion coefficient as a function of temperature at 1 bar: (a) Rigid classical force fields, and (b) Polarizable and *ab initio* force fields. Symbols denote MD studies that have considered more than 1,000 water molecules, without including any system size corrections in the calculation of the water self-diffusion coefficient. The black lines denote Speedy–Angel-type correlations of experimental data (solid line: experimental data of Holtz et al. [385] in the temperature range 273–373 K; dashed line: experimental data of Qvist et al. [147] in the temperature range 253–293 K). Sources for MD data: SPC, COS2/G2, and COS2/B2 using 1,024 H₂O (Stukan et al. [165]); SPC/E and TIP4P/2005 using 2,000 H₂O (Moultos et al. [173]); SPC, SPC/E, TIP4P and TIP4P/2005 using 2,048 H₂O (Guevara-Carrion et al. [139]); TIP4P/2005, TIP4P-TPSS, TIP4P-TPSS-D3, and TIP4P-Huang using 3,000 H₂O (Koster et al. [192]).

accurately the vapour–liquid equilibrium that also over-predicts the self-diffusion coefficient of water at 1 bar. On the other hand, for the subsequent modifications (i.e. SPC/E [39] and TIP4P/2005 [105]) the predictions of the self-diffusion coefficient of water at 1 bar are significantly improved.

Figure 5(b) shows that the MD simulations reported by Koster et al. [192], using the water force fields TIP4P-TPSS and TIP4P-TPSS-D3, with 3,000 molecules, significantly over-estimate the self-diffusion coefficient of water at 1 bar. No further discussion was presented by the authors for the poor performance regarding the self-diffusion coefficient of these models. It should be noted that both TIP4P-TPSS and TIP4P-TPSS-D3 are force fields that were derived (Spura et al. [175]) from *ab initio* MD simulations by means of an improved force-marching scheme. On the other hand, the MD simulations that were reported by Yu and Gunsteren [365], with the polarisable models COS2/G2 and COS2/B2, using 1,000 H₂O molecules, show good agreement with the experimental values [Figure 5(b)]. Similar behaviour is observed for the MD simulations that were reported by Stukan et al. [165] with the four-site, polarisable, SWM4-NDP (Lamoureux et al. [107]) water model, using 1,024 H₂O molecules.

The agreement between the experimental self-diffusion coefficient of water and those calculated with the ELBA coarse-grained model (as reported by Ding et al. [191]) deteriorates significantly for temperatures other than 298 K as clearly shown in Figure 6. Molinero and Moore [130] reported MD simulations of the self-diffusion coefficient of the mW coarse-grained model [130] and observed significant deviations from the experimental values. This observation was in good agreement with the work of Espinosa et al. [180]. The calculations using mW are also shown in Figure 6. The discrepancy between the two aforementioned coarse-grained models and the

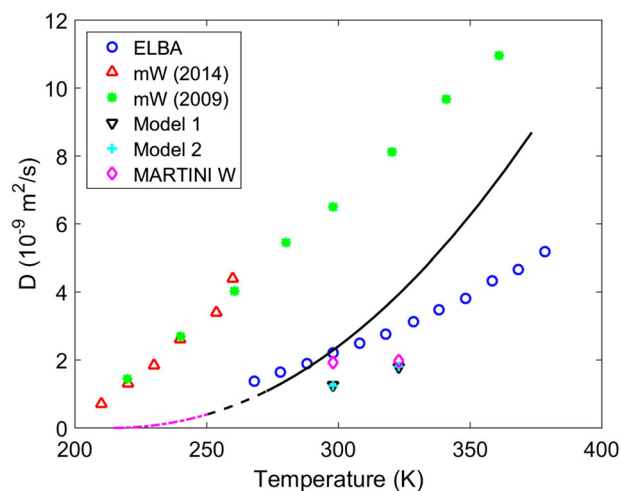


Figure 6. (Colour online) Water self-diffusion coefficient as a function of temperature at 1 bar for the coarse-grained water force fields ELBA (blue circles) reported by Ding et al. [191], mW (red triangles) reported by Espinosa et al. [180], mW (green stars) reported by Molinero and Moore [130]; and Model 1 (black triangles), Model 2 (cyan crosses) and MARTINI W (magenta diamonds) reported by Fuhrmans et al. [137]. The black lines denote Speedy–Angel-type correlations of experimental data (solid black line: experimental data of Holtz et al. [385] in the temperature range 273–373 K; dashed black line: experimental data of Qvist et al. [147] in the temperature range 253–293 K; dashed-dotted magenta line: extrapolation to lower temperatures of the correlation by Qvist et al. [147]).

experimental values can be further visualised by comparing the calculated values for the activation energy, E_a . The activation energy can be obtained from the slope of the line when we plot the self-diffusion coefficient in an Arrhenius-type plot. The self-diffusion coefficient data for ELBA, from Ding et al. [191], result in a value for the activation energy, $E_a = 9.998$ kJ/mol, while the data for mW, from Espinosa et al. [180], result in a value $E_a = 12.890$ kJ/mol. When the aforementioned MD-calculated values are compared against the experimental value, $E_a = 16.566$ kJ/mol, result in 39.7% and 12.6% errors for ELBA and mW, respectively. Correspondingly, the intercept, $\ln D_0$, has a value equal to -15.913 for ELBA and -13.460 for mW, resulting in 20.5% and 1.9% errors respectively, when compared with the experimental value of -13.207 .

2.3.2. The effect of supercooled conditions on self-diffusion coefficient

Figure 4 provides a plot of the water self-diffusion coefficient as a function of temperature at 1 bar, considering only the studies that have reported corrections accounting for system size effects. The same data are also used in Figure 7, in which the water self-diffusion coefficient is plotted as a function of the inverse temperature. Speedy–Angel-type correlations of the experimental data ([147,385]) are also shown in Figure 4. Furthermore, the MD data of the specific six studies have been correlated using three different types of equations. Namely, an Arrhenius (ARH) law given by:

$$D_{ARH} = D_0 \exp\left(-\frac{\alpha}{T}\right) \quad (4)$$

a Vogel – Fulcher – Tamann (VFT) equation:

$$D_{VFT} = \exp\left[\frac{-\alpha}{(T - \beta)} - \gamma\right] \quad (5)$$

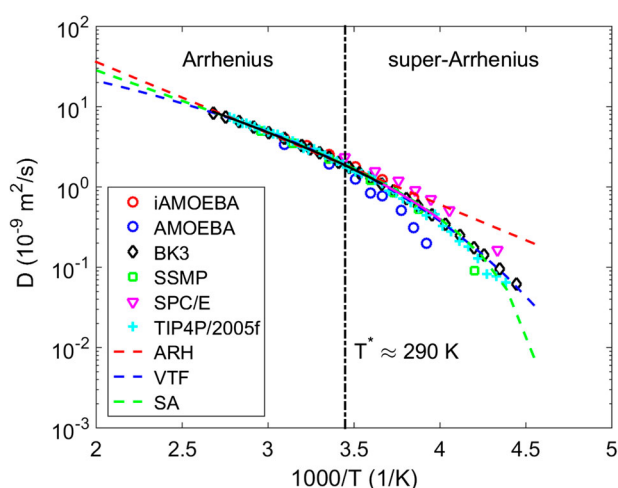


Figure 7. (Colour online) Water self-diffusion coefficient as a function of the inverse temperature at 1 bar. Symbol notation is the same as in Figure 4. The solid lines denote Speedy–Angel-type correlations of experimental data (black line: experimental data of Holtz et al. [385] in the temperature range 273–373 K; magenta line: experimental data of Qvist et al. [147] in the temperature range 253–293 K). The dashed lines correspond to correlations of all the MD data that included corrections based on system size effects. Colour code. Arrhenius (ARH) law: red line; Vogel–Fulcher–Tamann (VFT) equation: blue line; Speedy – Angel (SA) power law: green line.

and a Speedy – Angel (SA) power law described by the following equation:

$$D_{SA} = D_0 \left(\frac{T}{215.05} - 1 \right)^\gamma \quad (6)$$

where D_0 , α , β , γ are fit parameters given in Table 3. For the case of the Arrhenius law, $\alpha = E_a/R$, where R is the gas constant and E_a is the Arrhenius activation energy (in kJ/mol). In Table 3 the values for the percentage average absolute deviation (% AAD), defined as $\% AAD = 100 \times |(D^{calc} - D^{exp})/D^{exp}|$ are also shown. The superscripts *calc* and *exp* denote the calculated and experimental values of the self-diffusion coefficient of water respectively.

As can be seen in Figure 7 for temperatures higher than approximately 290 K the MD data for the water self-diffusion coefficient are in excellent agreement with the Arrhenius law, a behaviour known as ‘Arrhenius’. On the other hand, for temperatures lower than approximately 290 K significant deviations from the Arrhenius law begin to appear, a behaviour known as ‘super-Arrhenius’. The deviations become stronger as we enter deeper in the supercooled region (i.e. lower temperatures). For temperatures lower than 235 K (i.e. a region also known as ‘no man’s land’ [387]) the VFT-type equation seems to follow closer the MD self-diffusion coefficient data for the BK3 water force-field.

The value of the crossover temperature, $T_x = 290$ K, is obtained from the study of Xu et al. [388]. The authors presented experimental measurements for the self-diffusion coefficient of water and reported that the Stokes–Einstein (SE) relation, $D \sim (\tau/T)^{-1}$ (where τ is the translational relaxation time), breaks down for temperatures below T_x . The SE relation, which is regarded as one of the ‘hallmarks of transport in liquids’ according to ref [388], is replaced by the ‘fractional-SE’ relation, $D \sim (\tau/T)^{-t}$, for temperatures below T_x , with $t \approx 0.62$. Xu et al. [388] also reported MD simulations using the TIP5P [357] water force field and identified that the ‘fractional-SE’ relation, with $t \approx 0.77$, is applicable for temperatures lower than $T_x \approx 320$ K. The authors pointed out that the crossover temperature, T_x , seems to roughly coincide with the onset of the increase of the population of water molecules with LDA-like structure (i.e. low density amorphous solid water). At the same time a decrease occurs for the population of water molecules with HDA-like structure (i.e. high density amorphous solid water).

In the related literature ([11,388–390]) different values for the crossover temperature, T_x , have been used and consequently the discussion on where the ‘Arrhenius’ and ‘super-Arrhenius’ regions are located, can change accordingly. Let, for example, consider $T_x \cong T_S \approx 225$ K, which is the

Table 3. Parameters for the MD self-diffusion coefficient of water calculated using different correlations and % average absolute deviation (% AAD) between experimental data and correlations.

Correlation	D_0 (m ² /s)	a (K)	β (K)	γ	% AAD
ARH-type	2.1529×10^{-6}	2.0446×10^3	na	na	42.90
VFT-type	na	5.6714×10^3	149.4743	16.0620	5.91
SA-type	1.6035×10^{-8}	na	na	2.0255	7.61

na: not applicable.

temperature where thermodynamic and dynamic properties exhibit power law divergences. In that case, for $T > T_x$ the self-diffusion coefficient of water obeys ‘Arrhenius’ behaviour, termed also as ‘strong’ behaviour. On the other hand, for $T < T_x$ the self-diffusion coefficient of water obeys ‘super-Arrhenius’ behaviour, termed also as ‘fragile’ behaviour. Thus during cooling of water a ‘fragile’-to-‘strong’ (FTS) liquid transition will occur upon crossing T_x [389]. Alternatively, the extent to which the shear viscosity, η , deviates from the Arrhenius law, $\eta = \eta_0 \exp(-E/k_B T)$, constitutes the basis for classifying the liquids as either ‘strong’ or ‘fragile’ [11]. An FTS liquid transition has been reported by Starr et al. [79] who performed MD simulations for the self-diffusion coefficient of water using the SPC/E [39] force-field in a wide range of temperatures, T , and densities, ρ . Their study covered the following region of the $T - \rho$ plane: ($210 < T < 300$ K and $0.9 < \rho < 1.4$ g cm⁻³).

The behaviour of the self-diffusion of water at the super-cooled conditions and the connection to other water anomalies has attracted significant scientific attention. This issue has been addressed by both experimental and computational studies. Mallamace et al. [390] analysed experimental measurements in the pressure range 0.1–800 MPa and temperature range 252–400 K for the isothermal compressibility, K_T , defined as $K_T = -(\partial \ln \rho / \partial \ln P)_T$, and the coefficient of isobaric thermal expansion, α_P , defined as $\alpha_P = -(\partial \ln \rho / \partial T)_P$. The authors found that a temperature T^* exists ($T^* \sim 315 \pm 5$ K), such that K_T shows a minimum for all pressures considered. Furthermore, all the $\alpha_P(T)$ curves that are measured at different pressures cross at the cross-over temperature, T^* , resulting thus at a ‘singular and universal expansivity point’ with a value equal to $\alpha_P(T^*) \approx 0.44 \times 10^{-3}$ K⁻¹. The particular temperature T^* is the border between two distinct behaviours (indicating two distinct regions) that can be also clearly identified in the self-diffusion coefficient of water. Namely, for $T < T^*$ the self-diffusion coefficient of water has a maximum value that, as T increases, shifts to lower values of P and eventually disappears near T^* . This is the ‘super-Arrhenius’ region. On the other hand, for $T > T^*$ the self-diffusion coefficient of water has a more regular behaviour and obeys an Arrhenius law, shown in Equation (4).

Subsequently, we used the MD data from the six studies (at 1 bar) that have reported self-diffusion coefficient of water, accounting for corrections for system size effects, to calculate the corresponding parameters for an Arrhenius-type equation. Results for the fitting of each water force field separately are shown in Table 4, along with the combined fitting for all six

water force fields. Furthermore, we examine two different temperature ranges for fitting the MD data and we compare with the results obtained from experimental measurements. Namely, we consider: (i) the entire temperature range, and (ii) temperatures that are higher than approximately 270 K. In agreement with the previous discussion, we observe clearly that when we limit the fitting to the higher temperature range, a significant improvement is obtained upon comparison with the experimental data. From the six models considered in Table 4, the correlations of BK3 and iAMOEBA show better agreement with the experimental measurements for the self-diffusion coefficient of water at 1 bar, while the correlations of SPC/E and AMOEBA exhibit the highest errors.

Scala et al. [391] used the SPC/E [39] water force field to calculate the liquid entropy S , the vibrational entropy, S_{vib} , of the liquid constrained in one typical basin of the potential energy landscape, and the configurational entropy, S_{conf} , (defined as: $S_{conf} \equiv S - S_{vib}$) for the same state points considered in the earlier study of Starr et al. [79]. Scala et al. observed that both S_{conf} and D exhibit maxima which become more pronounced with decreasing temperature. Furthermore, they observed that the maxima occur at $\rho \approx 1.15$ g cm⁻³. Figure 8 clearly demonstrates the remarkable correlation between the qualitative behaviours exhibited by both S_{conf} and D . For the case of SPC/E water force field and the range of parameters examined, it was also found that the Adams-Gibbs equation, given as $D \sim \exp(-B/TS_{conf})$, holds.

An alternative approach to connect thermodynamic and dynamic (i.e. transport) properties of dense fluids is also provided by excess entropy scaling relationships for transport properties. The excess entropy, S_{ex} , is defined as the difference, $S_{ex} \equiv S - S_{ig}$, between the entropy of the fluid, S , and the entropy of the ideal gas, S_{ig} . Transport properties including diffusivity, viscosity and thermal conductivity can be conveniently reduced to dimensionless form using reduction factors based on kinetic theory. It has been shown, initially by Rosenfeld [392], and subsequently by others ([393,394]) that for a wide range of simple liquids the following semi-empirical scaling relationship is valid: $X^*(T) \sim \exp(b(\rho)S_{ex})$, where X^* denotes dimensionless transport properties, $b(\rho)$ is a T -independent parameter that depends on both the nature of the interactions and the transport property, and ρ is constant. Chopra et al. [395] used the following dimensionless, translational self-diffusion coefficient, $D^* = D((\rho/M)^{1/3}/(k_B T/M)^{1/2})$, where M is the molecular weight. S_{ex} accounts for all intermolecular correlations (i.e. two-, three-, and higher body). Chopra et al. considered also the simpler case of only the translational

Table 4. Parameters of fitting the MD self-diffusion coefficient of water at 1 bar, using an Arrhenius-type equation, for various water force fields.

Study	Model	T -range (K)	E_a (kJ/mol)	$\ln(D_o \text{ (m}^2\text{/s)})$	% AAD in E_a All T 's	E_a	$\ln(D_o \text{ (m}^2\text{/s)})$	% AAD in E_a $T > 270$ K
						(kJ/mol)	$T > 270$ K	
Qvist et al. [147]	SPC/E	230–290	19.978	–11.58	20.59	17.891	–12.46	8.00
Wang et al. [98]	iAMOEBA	260–323	17.148	–12.92	3.51	16.511	–13.16	0.33
Wang et al. [98]	AMOEBA	255–323	22.319	–11.17	34.73	20.842	–11.73	25.81
Kiss & Baranyai [179]	BK3	225–373	16.658	–13.19	0.56	15.912	–13.45	3.95
Tran et al. [189]	SSMP	238–338	18.508	–12.52	11.72	17.730	–12.80	7.03
Guillard et al. [194]	TIP4P/2005f	228–360	17.474	–12.87	5.48	17.346	–12.91	4.70
	Combined	225–373	17.247	–12.96	4.11	16.825	–13.11	1.56
Experimental: [147,385]		273–373	16.566	–13.21				

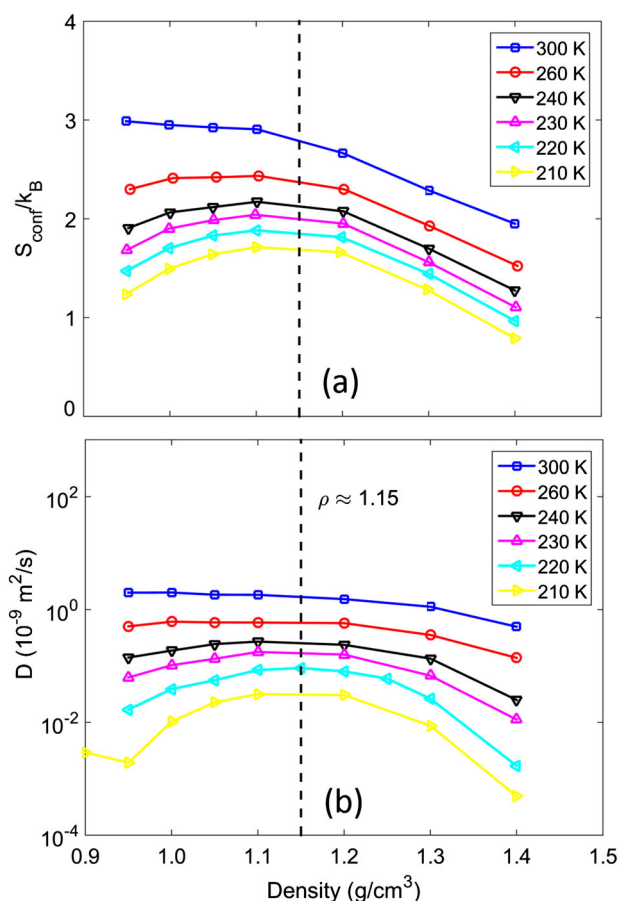


Figure 8. (Colour online) Density dependence for: (a) SPC/E water configurational entropy (Scala et al. [391]), and (b) water self-diffusion coefficient using SPC/E model (Starr et al. [79]). Symbols denote MD simulations for six isothermal paths (from top to bottom: 300, 260, 240, 230, 220, and 210 K).

contributions to the excess entropy and accounting only for the two-body contributions, $S_{(2)}$. The authors employed the SPC/E water force field and (i) confirmed the validity of the Rosenfeld-type scaling for the self-diffusion coefficient of water and (ii) confirmed the behaviour described by Starr et al. [79] in Figure 8.

Yan et al. [396] used the TIP5P [357] water model to investigate the relationship between the excess entropy and the anomalies of water. They found that the two-body excess entropy adequately predicts the regions of structural, dynamic, and thermodynamic anomalies of water as well as the location of the Widom line (see also Section 2.3.3. for additional details). In two recent studies, using the TIP4P water force field, Gallo et al. ([182]) and Corradini et al. ([188]) have shown that if S_{ex} is approximated with $S_{(2)}$, (i.e. the two-body term of the excess entropy), the same FTS transition of the diffusion coefficient is found. Namely, the aforementioned simulation studies indicate that the two-body term shows the FTS crossover and, therefore, captures the features of water behaviour also in the high-density side.

2.3.3. The effect of temperature on self-diffusion coefficient at high pressures

As discussed in the previous section, Mallamace et al. [390] analysed experimental measurements in the pressure range

0.1–800 MPa and temperature range 252–400 K, and pointed out the existence of a temperature T^* ($T^* \sim 315 \pm 5 \text{ K}$) that clearly identifies the border between two distinct behaviours for the self-diffusion coefficient of water.

Starr et al. [79] reported extensive MD simulations for the self-diffusion coefficient of water using the SPC/E [39] force-field in a wide range of temperatures, T , and densities, ρ . However, due to computational limitations they performed simulations with 216 water molecules. They also reported that no significant effect in their limited study of larger systems (i.e. 1,728 water molecules at 190 and 200 K and 1 g cm^{-3}) was observed. The discussion presented previously in Section 2.1 clearly indicates that at least 1,000 water molecules are required to significantly reduce the errors introduced by the finite system size effects. Subsequently, Mittal et al. [112], and Chopra et al. [395] performed similar simulations with a larger number (500) of SPC/E water molecules. The use of a larger system is expected to shift the calculated self-diffusion coefficient to higher values. Both studies were in reasonable agreement with the experimental behaviour described by Mallamace et al. [390].

Only a limited number of MD studies have considered the effect of pressure on the self-diffusion coefficient of water and simultaneously addressed adequately the issue of system size effects. Studies that provided corrected MD values for the water self-diffusion coefficient include Jiang et al. [190] who reported results using the HBP, BK3, and TIP4P/2005 water force fields, and Tran et al. [189] who reported results using the SSMP and TIP4P-Ew force fields. These studies explored the effect of pressure on the water self-diffusion coefficient for various isotherms. Kiss and Baranyai [179] used BK3 [160] and examined the effect of temperature on the water self-diffusion coefficient at 1,500 bar.

A number of studies, that used more than 1,000 water molecules, have also examined the effect of pressure on the self-diffusion coefficient of water, without providing any further corrections to the MD values, to account for system size effects. Xu et al. [106] used 1,728 ST2 water molecules, Guevara-Carrion et al. [139] used 2,048 TIP4P/2005 water molecules, Moulton et al. [173] used 2,000 SPC, SPC/E, and TIP4P/2005 water molecules. Furthermore, a detailed list of studies in which less than 1,000 water molecules were used can be found in the Supporting Information (Table SI-1).

To examine the applicability of the observation by Mallamace et al. [390] to the MD-calculated self-diffusion coefficient of water, we plot them as a function of pressure for various isotherms. As shown in Figure 9, the overall picture is consistent with the conclusions reported by Mallamace et al. [390]. We observe a weak dependence on pressure for the lower temperatures, which increases at higher temperatures. The agreement between the MD and the experimental values is better at lower temperatures, while deviations increase at higher temperatures. Figure 9(a) shows the pressure dependence of D for the HBP, BK3, SPC/E and TIP4P/2005 water force fields, at 298, 373, and 473 K. The MD data are compared with the experimental values reported by Krynicki et al. [289]. Figure 9(b) shows the pressure dependence of D for the TIP4P/2005 water force fields, at 260, 273, 280, 288, and 298 K (i.e. case with $T < T^*$). MD data are compared with the experimental data of Prielmeier et al. [292]. The MD data follow closely

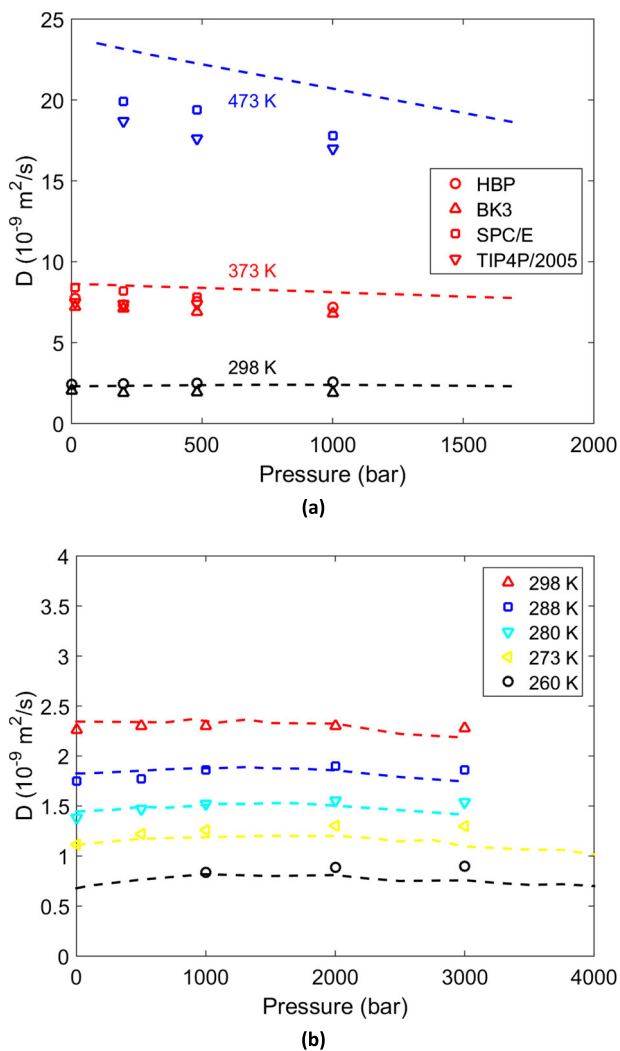


Figure 9. (Colour online) Self-diffusion coefficient of water as a function of pressure for various isotherms. Symbols denote the MD simulations and dashed lines denote experimental measurements. Lines and symbols of the same colour correspond to the same temperature. (a) MD data for HBP and BK3 water models are from Jiang et al. [190] (with corrections for system size effects included), while for SPC/E and TIP4P/2005 are from Moulton et al. [173] (using 2,000 water molecules). (b) MD data for TIP4P/2005 are from Guevara-Carrion et al. [139] (using 2,048 water molecules). Experimental values for (a) are from Krynicki et al. [289], while for (b) from Prielmeier et al. [292].

the experimental values and indicate the existence of a maximum value. The existence of the maximum in Figure 9(b) would be clearer if data at higher pressures were available.

To this purpose, in Figure 10 we show a plot of the MD simulation for various force fields at 298 K. For this temperature, MD simulations are available for pressures up to 10 kbar for the cases of TIP4P-Ew and SSMP, reported by Tran et al. [189]. Both water force fields exhibit a maximum for the self-diffusion coefficient at 298 K. Furthermore, excellent agreement between experimental values and MD simulations are found for the case of SSMP.

In addition to studying the effect of pressure and temperature on the self-diffusion coefficient under constant temperature or pressure conditions respectively, the behaviour of the self-diffusivity along the two-phase (i.e. Vapour – Liquid equilibrium, VLE) coexistence curve is also of interest. Figure 11 shows the available MD calculations of the self-diffusion

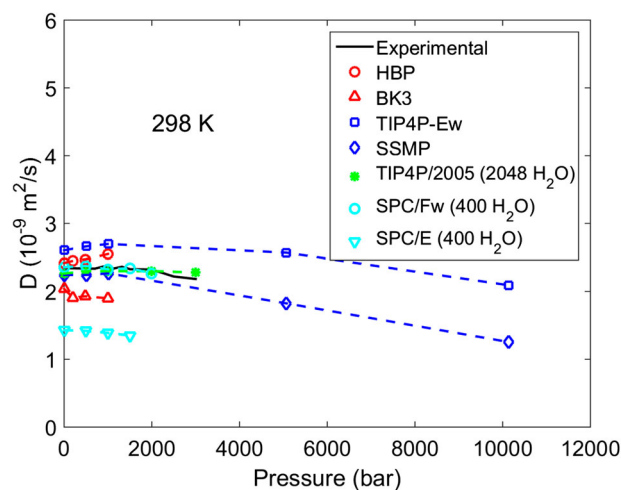


Figure 10. (Colour online) Self-diffusion coefficient of water plotted as a function of pressure at 298 K. Symbols denote the MD simulations and black solid line denotes experimental measurements (Prielmeier et al. [292]). The dashed lines connecting the MD data points are guides to the eye only. The MD data for HBP and BK3 water models (from Jiang et al. [190]) and for TIP4P-Ew and SSMP (from Tran et al. [189]) have included corrections for system size effects. Data for TIP4P/2005 are from Guevara-Carrion et al. [139] (using 2,048 water molecules), while for SPC/Fw and SPC/E are from Raabe and Sadus [148] (using 400 H₂O molecules).

coefficient plotted as a function of temperature, along the liquid branch of the VLE curve. The experimental data used for the comparison are from the work of Yoshida et al. [294].

Bauer and Patel [126] introduced the polarisable water force field TIP4P-QDP-LJ and used it to calculate water self-diffusion coefficient, among other properties. The reported values for self-diffusivity are corrected in order to account for system size effects. Figure 11 shows excellent agreement with the experimental values, for the entire range considered (i.e. up to 600 K). The model predicts the following critical properties: $T_c = 623 \text{ K}$, $P_c = 250.9 \text{ atm}$, and $\rho_c = 0.351 \text{ g cm}^{-3}$. These values should be compared against the experimental: $T_c = 647.1 \text{ K}$, $P_c = 218 \text{ atm}$, and $\rho_c = 0.322 \text{ g cm}^{-3}$.

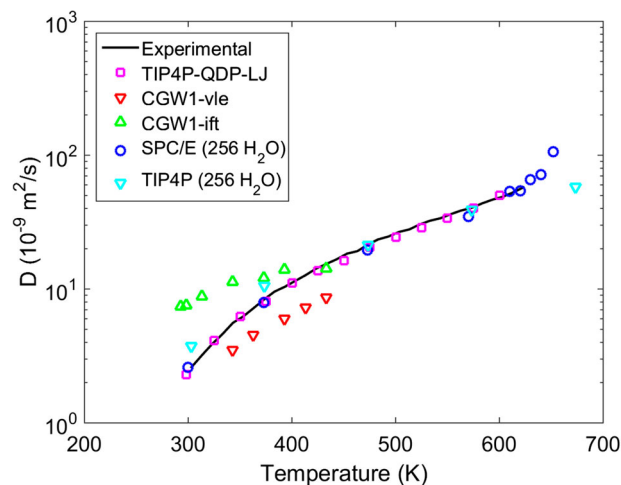


Figure 11. (Colour online) Self-diffusion coefficient of liquid water as a function of temperature along the VLE line. Symbols denote the MD simulations and black solid line denotes experimental measurements by Yoshida et al. [294]. Sources for MD data: TIP4P-QDP-LJ [126]; Mie (8-6) CGW1-vle and Mie (8-6) CGW1-ift [184]; SPC/E [59]; TIP4P [294].

In Figure 11 simulation data from two versions of the coarse-grained model introduced by Lobanova et al. [184] are also shown. The model employs a single interaction site (bead) to represent a water molecule. Based on the use of different target properties during the parameter optimisation two versions were introduced. Namely, the Mie (8-6) CGW1-vle model was parameterised to match the saturated-liquid density and vapour pressure; while the Mie (8-6) CGW1-ift model was parameterised to match the saturated liquid density and vapour-liquid interfacial tension. The authors attributed the overestimation of the water self-diffusion coefficient by the Mie (8-6) CGW1-ift model to the fact that the coarse-grained models have a higher mobility since the water molecules are not slowed down by the re-orientation of the hydrogen atoms and the formation/break-up of hydrogen bonds. Significant over-estimation of the diffusion coefficient occurred at low temperatures, and became comparable with the experimental values at the higher-temperature limit considered (approx. 350–400 K). On the other hand, the authors attributed the under-estimation of the water self-diffusion coefficient by the Mie (8-6) CGW1-vle model to the fact that the large values of the energetic well of the potential, resulting from the use of the vapour pressure as the target property. A third version was also developed, Mie (8-6) CGW2-bio, where two water molecules were considered per coarse-grained bead. For the particular version only a single value at 298 K and 1 bar has been reported (see also Table 2).

Finally, the simulations reported by Guissani and Guillot [59] using 256 SPC/E [39] water molecules, and by Yoshida et al. [294] using 256 TIP4P water molecules are shown also in Figure 11. Very good agreement is observed between the MD simulations and the experimental values for both the SPC/E and TIP4P water force fields. However, no corrections for system size effects were included in the reported self-diffusion coefficient. Therefore, upon inclusion of the corrections a shift to higher values is expected for both SPC/E and TIP4P, resulting eventually in the over-estimation of the self-diffusivity. This behaviour is consistent with the discussion presented in Sections 2.1 and 2.3.1 (see also Figures 4 and 5(a)).

The study of diffusion phenomena at near-critical or supercritical conditions for water is significant for geological processes. Despite their importance, only a limited number of simulation studies have explored this region for the case of water. Nieto-Draghi et al. [92] calculated water self-diffusion coefficient for the following four force fields: TIP4P [32], TIP5P [357], SPC/E [39], and DEC [87]. In all simulations they used 256 water molecules. They reported good agreement at high densities (e.g. between 2% and 5% at $\rho = 0.65 \text{ g cm}^{-3}$), while the highest disagreement ($\approx 15\%$) was found for the low densities and was attributed to the lack of polarizability of the models. For all force fields considered, over-predictions of the self-diffusivities were observed. Please note that the deviations are expected to increase further, if corrections for system size effects are incorporated. Shvab and Sadus [187] reported calculations for water self-diffusion coefficient using the TIP4P/2005 [105] and TIP4P/2005f [141] force fields, at 670 K, using 1,728 H_2O molecules, without corrections for system size effects. They found better agreement for the flexible force field. The rigid force field was found to underestimate the water self-

diffusion coefficient by approximately 2–10% in the first half of the density range. They attributed the higher values of TIP4P/2005f to the elongated O-H bond, which results in a higher dipole moment. Yoshida et al. [116] reported self-diffusivities using 1,000 TIP4P H_2O molecules, at 673 K, without corrections for system size effects. On the other hand, Tainter et al. [183] calculated water self-diffusion coefficient using the E3B3 (which accounts for three-body interactions) and TIP4P/2005 [105] force fields at 673 K, with their study also accounting for system size corrections. The authors used experimental values for the shear viscosity to correct for finite-size effects, instead of using MD-calculated values, as already discussed earlier.

Figure 12 shows a comparison of the MD-calculated values for the water self-diffusion coefficient, using the aforementioned models, with the experimental measurements reported by Lamb et al. [290]. The authors measured experimentally the self-diffusion coefficient of compressed supercritical water as a function of pressure, in the temperature range 673–973 K, using the NMR spin-echo technique. The specific experimental data are probably the only available water self-diffusion data at supercritical conditions. For all four models considered, we observe a good agreement between experimental and MD values for the self-diffusivity, especially for densities that are higher than the critical density.

Gallo et al. [182] in a seminal study used available experimental data and performed extended MD simulations with the TIP4P/2005 water model (4,096 water molecules), to study the thermodynamic properties of water in the temperature range 600–800 K and the pressure range 175–400 bar. They demonstrated that the lines connecting the maxima of the response functions (i.e. the constant pressure-specific heat, C_p ; the isobaric thermal expansion coefficient, α_p ; and

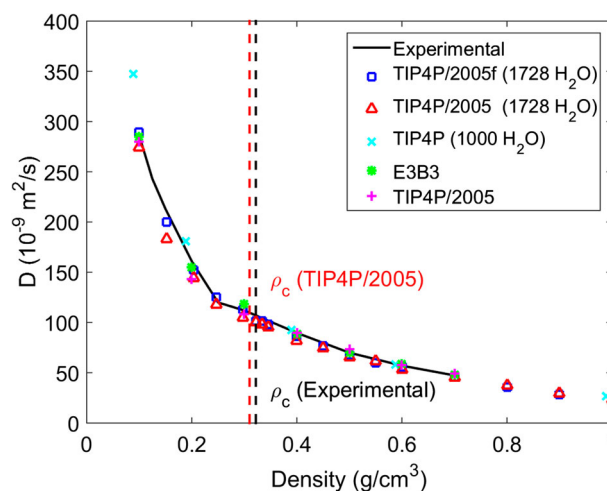


Figure 12. (Colour online) Self-diffusion coefficient as a function of density for supercritical water along the isotherm of 673 K. Symbols denote the MD simulations and black solid line denotes experimental measurements by Lamb et al. [290]. The vertical dashed lines denote the critical density values. Experimental (black): $\rho_c = 0.322 \text{ g cm}^{-3}$; TIP4P/2005 (red): $\rho_c = 0.31 \text{ g cm}^{-3}$. Sources for MD data: E3B3 and TIP4P/2005 (magenta cross) are at 673 K from Tainter et al. [183] with system size corrections incorporated. TIP4P/2005 (red triangles) and TIP4P/2005f are at 670 K from Shvab and Sadus [187] using 1,728 H_2O molecules, while TIP4P are at 673 K from Yoshida et al. [116] using 1,000 H_2O molecules, without any further corrections for system size effects.

the isothermal compressibility factor, K_T) converge in a single line (i.e. Widom Line – WL) as they approach the critical point. Note that a similar WL has also been found in the deeply super-cooled region.

The WL, found in the supercritical region, delineates a crossover from liquid-like to gas-like behaviour. This behaviour is clearly visible in other transport properties as well. For example, if we plot the shear viscosity as a function of temperature, for various isobars, we can observe that in the liquid-like portion, all curves show a strong decrease of viscosity with temperature. In the gas-like portion, the change of slopes is not as strong. The same picture was obtained by Galo et al. [182] for the case of the inverse self-diffusivity of TIP4P/2005 [105] water. In a subsequent study, Corradini et al. [188] extended the previous analysis to TIP3P [32], TIP4P [32], TIP5P [357], and SPC/E [39] water force fields and obtained similar behaviours.

3. Self-diffusion coefficient of water in confinement

The self-diffusion of confined water has been evaluated in the recent literature for a variety of confining systems. These systems constitute of materials differing in their chemical nature, shape, size, and surface charge distribution, features that significantly impact structural and transport properties of the confined fluid near the interface. Carbon compounds, minerals, zeolites, gold plates, surfactants, and biomolecules have been employed as the confining material in calculating water self-diffusion coefficient via MD simulations. Figure 13 presents the distribution of published articles in the open literature (in %, out of 109 papers) with calculated self-diffusion coefficient of water in different confining materials, showing the predominance of minerals and carbon compounds (see also Table SI–3 of the Supporting information).

3.1. Carbon compounds

Most of the data found in the literature are related to carbon compounds as the confining material. Usually analysed at room temperature, water self-diffusivity is commonly calculated through Einstein's and Green-Kubo's method using mostly the SPC/E [39] force field, but also SPC [355], TIP3P

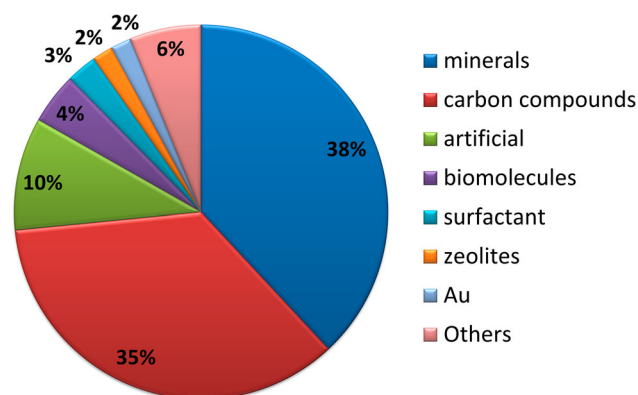


Figure 13. (Colour online) Distribution of published articles in the open literature (in %) with calculated self-diffusion coefficient of water in different confining materials.

[32], and variations of TIP4P [32]. The values for water self-diffusion coefficient differ considerably even between the same confining material depending on density, temperature, and size of confinement.

Striolo [198] has proposed that the diffusion of water in carbon nanotubes can be described by three different mechanisms depending on the time evolution of the mean squared displacement. When water molecules move in a chaotic manner and overcome one another in the direction of motion, the mean squared displacement varies linearly with time, which entails a Fickian regime. Nevertheless, when water molecules are confined in such a way that resembles an one-dimensional path, the mean squared displacement scales with the square root of time, and such a mechanism is called single-file diffusion. The intermediary mechanism is characterised by a ballistic regime where the mean square displacement is proportional to the square of time. In a subsequent work, Striolo [199] has shown that water diffusion in a carbon nanotube doped with carboxyl group (which makes the surface hydrophilic) obeys different mechanisms compared to water diffusion in a pure hydrophobic carbon nanotube. Moreover, the self-diffusion coefficient of water is significantly lower in the doped carbon nanotube.

Geometry is a key factor on transport properties of confined fluids. Nie et al. [200] calculated SPC/E [39] water self-diffusion coefficient in carbon nanotubes built with three different geometries for the cross-sectional area: circular, square, and triangular. By varying the chirality of the nanotube, the same trend is observed for all three different geometries, finding the lowest self-diffusion coefficient values for water molecules confined by a CNT (8,8), although the values are different for different cross-sectional areas.

A question that might emerge in these calculations is how one can separate the effect of the interface and the effect of confinement. Zheng et al. [201] investigated such a limit using TIP4P-Ew water molecules within carbon nanotubes. They claimed that the effect of the confinement is relevant for nanotubes up to 16 Å of diameter. The volume fraction, θ , of water molecules that feel the interactions with the wall constitutes a scaling parameter for the water self-diffusion coefficient in confinement. Chiavazzo et al. [202] showed that the relation between the self-diffusion coefficient of water within carbon nanotubes and the bulk water self-diffusion coefficient scales linearly with θ .

Martí and Godillo [203] analysed the SPC/E [39] water self-diffusion coefficient in carbon nanotubes with different chiralities at high temperatures (between 573 and 773 K). The logarithm of such self-diffusion coefficient depends almost linearly with the inverse of temperature, especially for CNT (10,10) and CNT (12,12), which shows that an Arrhenius behaviour may also be present in confinement.

Investigating spatial variation of the diffusion coefficient and its directional components, Farimani and Aluru [204] calculated the diffusion coefficient for SPC/E [39] water confined by (10,10), (20,20) and (30,30) carbon nanotubes and noticed that diffusion enhancement is evident near the surface for all studied cases. The spatial variation of axial diffusion coefficient depends on the size of the nanotube, being sharper in the (20,20). As the diameter increases, a bulk-like region is

observed at the centre of the nanotube and the effect of surface diminishes as expected. For carbon nanotubes with diameter $d < 2.2$ nm, the average axial diffusion coefficient is lower than the bulk because confinement plays a dominant role. For $2.3 \text{ nm} < d < 6.0$ nm, diffusion coefficient is higher than the bulk one, reaching a maximum at $d = 2.7$ nm due to surface contribution to depletion of hydrogen bonds and the existence of a bulk region for normal diffusion of molecules. For $d > 6.0$ nm, the average self-diffusion coefficient is close to the bulk value. The average axial self-diffusion coefficient for carbon nanotubes with different diameters is shown in Figure 14. Data from Liu and Wang [205] are also included for comparison, showing some differences between the two works. As the carbon nanotube diameter increases, the water self-diffusion coefficient approaches the bulk value.

Farimani and Aluru [204] also presented an evaluation of the diffusion mechanisms described previously (Striolo [198]) and claimed that for diameters $d < 1.5$ nm the diffusion mechanism is non-Fickian; i.e. it might be either a transition state (for the (7,7) carbon nanotube) or single-file diffusion, in the case of (8,8) nanotube. For $1.6 \text{ nm} < d < 2.3$ nm and $d > 4.0$ nm, Fickian diffusion is observed. When $2.4 \text{ nm} < d < 4.0$ nm, a transition between a Fickian and a ballistic mechanism is observed.

Carbon compounds were also widely studied as slit pores in the form of parallel sheets of graphite (Hirunsit and Balbuena [206]; Sanghi and Aluru [207]) and graphene (Mozaffari [208]; Muscatello et al. [209]). Sendner et al. [210] confined water between plates of a diamond-like structure and analysed the perpendicular diffusion coefficient as the surface hydrophobicity was changing. Using the SPC/E [39] force field, they found that when the material becomes more hydrophilic, surface binding and trapping of water alter the pure diffusive regime observed previously.

Nguyen and Bhatia [211] studied water dynamics in activated carbon fibres, due to their importance on adsorption-based processes. The authors tried to capture the influence of

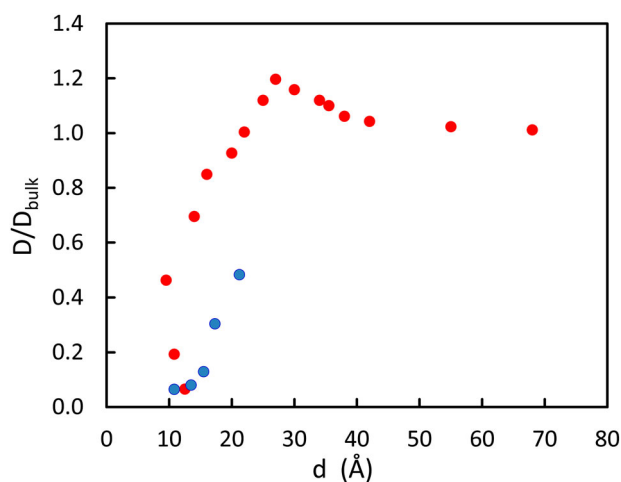


Figure 14. (Colour online) Ratio between axial self-diffusion coefficient of water confined in carbon nanotubes and bulk water self-diffusion coefficient as a function of the carbon nanotube diameter. Blue circles, 298 K, $1000 \text{ kg}\cdot\text{m}^{-3}$, SPC water model (Liu and Wang, [205]). Red circles, 300 K, $1000 \text{ kg}\cdot\text{m}^{-3}$, SPC/E water model (Farimani and Aluru, [204]).

structural disorder and to create a more realistic model to evaluate water diffusion on nanoporous carbons. A transition between Fickian and single-file diffusion mechanisms that depend on the temperature was found. They observed that the self-diffusion coefficient increases with the temperature and is higher for lower adsorption loadings. Diallo et al. [212] also simulated water confined by activated carbon fibres. They evaluated the diffusion coefficient of supercooled water ($220 \leq T \leq 280$ K) and compared the results with experimental data from quasi-elastic neutron scattering. They concluded that the self-diffusion of confined water is lower than the self-diffusion coefficient of bulk water, but comparable to water in carbon nanotubes and other porous media of similar pore size.

Martí et al. studied the dynamic properties of water confined between graphite (Gordillo and Martí [213]) and graphene (Martí et al. [214]) plates using a flexible SPC water force field and evaluated the changes with temperature. In other studies, they calculated the diffusion coefficient for SPC water at different densities (Martí et al. [215], Tahat and Martí [216], Martí et al. [217]), showing its evolution with a growing distance from the surface. Mosaddeghi et al. [218] also investigated the confining effect of graphite on the water self-diffusion coefficient by changing the density and the slit pore size. The methods used to calculate the diffusion of SPC/E [39] water were Green-Kubo and Einstein's and the results were comparable, with restrictions for smaller sizes due to high oscillations of the velocity auto-correlation function.

Graphite was also used as a hydrophobic model for biomaterials. Surface properties influence material performance and their understanding is extremely important for biomedical applications (Spera et al. [219]). Water-surface interaction has considerable influence on the biocompatibility of implant materials (Wei et al. [220]), macromolecular association and protein assembly (Choudhury and Pettit [221]). Wei et al. [220] used MD simulations to understand the difference between biocompatibility of carbon (in graphite form) and TiO_2 . They found that diffusion of SPC/E [39] water on graphite is higher than on titanium oxide due to the stronger interaction between water and TiO_2 surface, which could explain the greater affinity of the human organism with this material once the cells would interact with water instead of the material directly. This work showed that the surface chemistry has more impact on the diffusion of water compared to the slit pore size.

Kim et al. [222] reported the self-diffusion coefficient of SPC/E [39] water confined between two graphene plates and between plates of graphene and mica at the opposite ends of confinement. The presence of different surface features give rise to competition between ordering induced by water interaction with mica and pure diffusive flow induced by graphene.

3.2. Minerals

This important class of materials covers silica, clays, mica, hydroxyapatite, rutile and other known minerals. They are extremely relevant to a wide variety of processes, such as catalysis and separation (Spohr [223]), nanofluidics (Leng and Cummings [224]) and in the food and cosmetic industry (Portion et al. [225]). Particularly the presence of water gives rise to

interesting phenomena, e.g. interfacial water tends to form hydrogen bonds with hydrophilic mineral surfaces, ordering the water layers and reducing diffusion (Ou et al., [226]).

Magnesium oxide [$\text{Mg}(\text{OH})_2$] shows a potential for use in water environment remediation and industrial water treatment. Although magnesium oxide has a hydrophilic nature, unlike most minerals, Ou et al. [226] observed a modest effect on the dynamic behaviour of water near the $\text{Mg}(\text{OH})_2$ confining surface and no adsorption sites. Their study with flexible SPC water found self-diffusion coefficient in the same order of magnitude as bulk water. They have also shown that the parallel diffusion is twice the value of the perpendicular diffusion, corroborating that water moves more freely in the unconfined directions, as expected.

The confinement of water between mica surfaces, which are highly hydrophilic, has an important relation to biolubrication, ion channels and clay swelling (Leng and Cummings [224], Li et al. [227]). Leng and Cummings [224] studied TIP4P water confined between two parallel mica surfaces at different pressures, 1 and 150 bar, and noted the same behaviour for both cases: significant drop of the diffusion coefficient near the wall to roughly four orders of magnitude lower than bulk value, indicating strong interactions of water with mica.

Feldspar, a mineral that hosts contaminants such as uranium within its intra-grain fractures, was used in the MD study by Kerisit and Liu [228] as confining material to study the self-diffusion coefficient of SPC/E [39] water. The value of the parallel diffusion coefficient increased with the distance from the surface, while the perpendicular one has a behaviour related to the density profile. Computing the average self-diffusion coefficient, they discovered the presence of an interfacial region 2.0–2.5 nm wide, where the self-diffusion coefficient in confinement is significantly smaller than in the bulk phase and that surface effects only become negligible for confinement width of several tens of nanometres.

The major component of carbonate rocks is calcite, an important mineral for CO_2 sequestration, oil exploration, and other geological processes. Mutisya et al. [229] found that the water dynamics are affected by the interaction between water and calcite surface reducing the self-diffusion coefficient and inducing water layering. The calculation of the parallel coefficient was performed according to the method of Liu et al. [230], using a flexible SPC/Fw water model. Mutisya et al. [229] found values smaller than the bulk self-diffusion for pores ranging from 1.0 to 6.0 nm wide, with confinement effects enhanced for the narrowest pore due to overlap of surface effects.

The interaction with the material surface can affect the local environment and modify water dynamics under confinement. This has been investigated by Prakash et al. ([231,232]) for hydroxyapatite (i.e. a component of bone mineral phase which is used as scaffold for bone repair). Prakash et al. [232] characterised water transport properties by MD simulations applying different water potentials and found that the SPC/E [39] water together with the core-shell potential for hydroxyapatite is the most accurate combination for predicting diffusion properties. With these models, Prakash et al. [231] calculated the anisotropic self-diffusion coefficient of the second-order diffusion tensor and found that the perpendicular component

is significantly lower than the parallel ones for all the studied widths. The calculation of transport properties showed a dependency on the size of the nanopore, confirming the work of Pham et al. [233], which showed this behaviour for water confined in hydroxyapatite pores from 2.0 to 6.0 nm wide at different temperatures.

Titanium dioxide (TiO_2) is present in many applications such as photo-catalysis, solar cells, optical sensors, bone implants, and biomedical coatings. Předota et al. [234] confined water in a TiO_2 slit pore and analysed the axial profile of parallel and perpendicular self-diffusion coefficient of SPC/E [39] water at 298, 448, and 523 K. The diffusion coefficient was shown to increase with temperature and, for all cases, the perpendicular component was found to be smaller than the parallel one. In the same study three regions between the confining walls were identified: the first layer near the surface where the self-diffusion coefficient is nearly zero, an inhomogeneous area where the diffusion changes with the surface distance, and a bulk-like region beyond a distance of 1.5 nm from the walls. Solveyra et al. [235] and Cao et al. [236] studied SPC/E [39] water self-diffusion inside rutile nanopores with different diameters and found that the self-diffusion coefficient are significantly reduced near the surface due to strong bonding with water. Solveyra et al. [235] suggested that, due to the first compact monolayer of water formed near surface, it is possible to compare the results with a less hydrophobic material of smaller radius.

Several works use silica as confining material to study water dynamics due to this mineral's importance in catalysis and separation technology. Either as parallel planes or cylindrical pores, self-diffusion of water was analysed to assess water behaviour with changes in pore size (Zhang et al. [237], Renou et al. [238], Dickey and Stevens [239]), temperature (Ishikawa et al. [240], Patsahan and Holovko [241]), surface composition (Siboulet et al. [242], Jeddi and Castrillón [243], and Lerbret et al. [244]), and water content (Spohr et al. [223]). The results show that, due to its hydrophilic nature, silica has a strong interaction with water which significantly decreases the diffusion coefficient near the surface due to partial adsorption of water layer near the walls. This effect was also noticed for higher temperatures. The diffusion coefficient increases with temperature, hydration, and with pore size, but decreases with density (Patsahan and Holovko [241]).

Silica can be also found as calcium silicate hydrate, which is present at the construction industry, as it is important for the strength, cohesion, and durability of the cement paste. Qomi et al. [245] analysed how different compositions of calcium and silicon affect physicochemical properties of water confined in these hydrophilic media. The self-diffusion coefficient was found to increase with increasing density. This anomalous behaviour is explained by a decrease on the diffusion energy barrier, which is the activation energy required for a water molecule to escape its dynamical cage. The mobility of water near the walls was strongly composition dependent and much slower than in the bulk phase due to strong interactions with the surface. This behaviour was confirmed by Hou and co-workers ([246–248]).

Another class of minerals is formed by clays. Mass transfer through clay nanopores is important for groundwater

hydrology, petroleum and gas engineering, and environmental applications (Boek [250], Boğan et al. [251]). Boğan et al. [251] employed the method by Liu et al. [230] to calculate the diffusion of SPC/E [39] water inside Na-montmorillonite pores from 2.0 to 9.0 nm wide and found that the self-diffusion at 300 K is reduced to 70% of the bulk value near the walls due to the higher density and surface effects. Boek [250] studied the parallel self-diffusion of water in montmorillonite for the cases of sodium, potassium, and lithium as the monovalent cation using the TIP4P water force field. He found smaller values of the diffusion coefficient for K-montmorillonite in comparison to the other metals. Rao et al. [252] also analysed water inside Na-montmorillonite and showed results for higher pressures and temperatures.

Other types of clays were also used as confining media for studying water dynamics: Zhou et al. [253] built sepiolite cells and showed that water confined inside this magnesium-rich clay has a much lower self-diffusion coefficient compared to water confined in montmorillonite. Smirnov and Bougeard [254] investigated SPC water dynamics between kaolinite surfaces, where the diffusion coefficient was calculated to be less than 5% of the bulk value near the walls. Michot et al. [255] evaluated SPC/E water diffusion confined between saponite, for different temperatures (i.e. 250–350 K) and obtained Arrhenius plots for the parallel component of the diffusion tensor.

3.3. Biomolecules

Stanley et al. [256] performed MD simulations to study the relation between dynamic transitions of biomolecules and dynamic properties of water. The TIP5P [357], and ST2 [28] potentials were chosen to describe water confined by lysozyme and DNA. It was shown that the self-diffusion coefficient of water exhibits Arrhenius behaviour at lower temperatures and a crossover to non-Arrhenius behaviour at approx. 245 K. The possibility that protein glass transition results from a change in behaviour of hydration water was stated in the same study. Sega et al. [257] investigated the diffusion behaviour of water close to a protein (GME ganglioside), considering the anisotropic nature of the fluid diffusion. For SPC water, they found that the parallel component is higher than the perpendicular one and both of them are one order of magnitude lower than the bulk near the protein surface.

Interested in chitosan/chitin films for food packaging, McDonnell et al. [258] evaluated the effects of increasing humidity on properties such as solvation, oxygen permeability, and diffusivity. Concerning the self-diffusivity of TIP4P water, they found an increase of one order of magnitude when the relative humidity varied from 15% to 95%. A strong O₂ attraction to protonated amine groups is overcome by water self-diffusivity, which means that reducing the latter will reduce the overall oxygen permeability.

Hua et al. [259] studied water dynamics to understand the kinetics of hydrophobic collapse and molecular self-assembly on biological environment. SPC water confined between BphC enzyme, a two-domain protein, showed lower self-diffusivity near the surface. Its mobility was also affected by surface geometry, hydrophobicity, and size of confinement – for

domain separation of 2.0 nm, the water behaviour was bulk-like at the centre of the inter-domain region.

3.4. Other confining media

Data are also available for theoretical confining media and some less frequently used materials, which are summarised in this section. Other confining materials with available self-diffusion coefficient data are ionomers (Berrod et al. [260]), aluminum phosphate nanotubes (Gavazzoni et al. [261]), polyamide RO membranes (Ding et al. [262]), boron nitride nanotubes (Won and Aluru [263]), and surfactants such as Newton Black films (Di Napoli and Gamba [264]).

Several works are dedicated in the study of dynamical properties of water confined between general hydrophobic/hydrophilic media described by LJ potential. Beckstein and Samson [265], Brovchenko et al. [266], Cui [267], Yamashita and Dai-guji [268], and Köhler et al. [269] confined water inside a cylindrical pore and analysed the influence of properties such as density, temperature, and pore radius on water self-diffusion. The authors agreed that hydrophilic walls slightly decrease diffusion in comparison to the bulk value, while hydrophobic walls can increase water self-diffusion up to three times the bulk value. The parallel and perpendicular components were also considered and for all cases the value was higher for the parallel component. Brovchenko et al. [266] found that the perpendicular components are closer in value to the parallel ones if the confining media is hydrophobic.

Kumar and co-workers ([270,271]), Bai and Zheng [272], and Choudhury [273] studied water under parallel plates. They evaluated the behaviour with temperature changes, density variations, high pressure and hydrophobic/hydrophilic nature. Bauer et al. [274] used different water force fields for the calculation of self-diffusivity inside hydrophobic plates and found that TIP4P showed an enhancement on the parallel component of the diffusion coefficient relative to bulk. This was explained based on a reduction on the molecular dipole moment of water in comparison to the average bulk value, weakening the intermolecular interaction of confined water and enhancing diffusion. Han et al. [275] observed a transition from a ballistic to a diffusive regime for TIP5P [357] water confined within hydrophobic parallel plates at different temperatures.

Different geometries were also considered as confining media for studying water dynamics. Marañón Di Leo and Marañón [276] confined SPC/E [39] water within rectangular prismatic nanotubes and calculated values for parallel and perpendicular components of the diffusion coefficient for water in both hydrophilic and hydrophobic walls, considering SPC/E bulk water diffusion value as 2.265×10^{-9} m²/s. These microporous crystalline structures have high selectivity, chemical stability and mechanical strength, and therefore are widely used as membranes for adsorption. Han et al. [277] evaluated kinetic and structural properties of TIP4P-Ew water confined inside 1-D and 3-D pore zeolites and studied the self-diffusivity to get insights on the effect of confinement in water dynamics, finding that the self-diffusion coefficient inside 1-D hydrophobic pores zeolites was approximately one order of magnitude higher than the self-diffusivity computed in the 3-D

pores. Shirono and Daiguji [278] calculated water's self-diffusion coefficient inside zeolites considering the polarisation of water by using the SPC-FQ potential. The calculated value agreed with the SPC/E calculations and the experimental data and they concluded that the variation of the dipole moment does not affect the dynamic properties.

Ju et al. [279] analysed the effect of pore width on water confined between two parallel Au plates at 400 K. Using the F3C [76] water potential, it was shown that for all plate distances the parallel component of the diffusion coefficient was larger than the perpendicular one but both increased with the gap size. Due to the interaction between water and Au atoms, the molecules near the surface were adsorbed forming a water layer, while for the largest gap (2.5 nm) the central region showed bulk-like behaviour.

Lane et al. [280] used gold as a substrate to study the properties of confined water between self-assembly monolayers (SAMs) of alkanethiols. SAMs are often used on surface modification to control surface interactions at the atomic level and are very important for nanofluidics and biomedical systems. They simulated water dynamics with the SPC/E [39] potential at 300 K and showed that there is an increment in the diffusion coefficient increasing water thickness. They concluded that geometry and water ordering, due to surface interaction, reduce diffusion by a factor of 100 in comparison to bulk water.

3.5. Methods and system size effect

The usual way to calculate the self-diffusion coefficient through MD simulation data is by applying either Einstein, or its analogue, Green-Kubo method. Such an approach is a possibility to interpret the time evolution of the particles mean squared displacement, or the time integral of the velocity auto-correlation function. This possibility is restricted to some assumptions that are frequently overlooked. The most important of these restrictions is the fluid density homogeneity. Although this is the case for bulk systems, for confined media such a hypothesis is invalid. The solid walls impose an inherent inhomogeneity on the confined fluid. This spatial variation of the fluid density inside the pore must be considered, especially close to the wall surface where the magnitude of such a variation can be extremely large. Moreover, for a confined fluid, the self-diffusion coefficient is no longer a simple scalar, but a diagonal second-order tensor, with components differing in different directions (Franco et al. [281]).

Notwithstanding the exposed rationality, in most of the literature, we continue to observe the employment of the Einstein, or Green-Kubo, method to calculate self-diffusion coefficient of confined fluids. There have been some developments of new methods to calculate the self-diffusion coefficient of confined fluids, considering the tensorial nature of such a coefficient and the intrinsic inhomogeneity of the confined media (Liu et al. [230], Franco et al. [282], Mittal et al. [283], von Hansen et al. [284], Carmer et al. [285]).

As well as for the bulk fluid, the system size effect in the calculation of the self-diffusion coefficient within MD simulations with periodic boundary conditions must be taken into account. Recently, Simonnin et al. [286] derived analytical expressions that consider the hydrodynamic effects between periodic

Table 5. Aspect ratio (H/L) for confined SPC/E water self-diffusion coefficient in different minerals at 300 K.

Ref.	Mineral	$D_{\text{parallel}}/D_{\text{bulk}}$	H/L
Kerisit and Liu [228]	Feldspar	0.817	1.95
Kerisit and Liu [228]	Feldspar	0.913	3.89
Ou et al. [226]	Mg(OH) ₂	0.494	3.30
Mutisya et al. [229]	Calcite	0.574	0.56

images for LJ particles confined within slit-pores. They found that the finite-size effects are minimised in elongated boxes (for a ratio of approximately than 2.8 between the height, H , and the length, L). Nevertheless, for other pore geometries, no correction for finite-size effects in confinement is currently available in the open literature to the best of our knowledge. Table 5 shows the ratio H/L for several calculations of the confined water parallel self-diffusion coefficient in different minerals at 300 K.

4. Conclusions and future outlook

In the current review we presented a detailed overview of molecular scale simulation studies examining the self-diffusion coefficient of water. In Section 2 we discussed issues related to the self-diffusion coefficient of water in the bulk phase, while in Section 3 we discussed the effect of confinement on the self-diffusion coefficient of water.

Numerous researchers, utilising a wide range of different force fields (e.g. rigid, flexible, polarisable, *ab initio*, etc.) have calculated the water self-diffusivity at a limited number of state points. However, only a handful of studies have performed a consistent and systematic exploration of the $P - T$, or $P - \rho$ plane. The particular problem is further exacerbated by the common practice of using a few hundred molecules, which can lead to a significant deviation between the simulated (i.e. finite system size) and real (i.e. thermodynamic limit) self-diffusivity. A notable exception is the recent works of Gallo et al. [182], and Corradini et al. [188] who considered the TIP4P/2005, TIP3P, TIP4P, TIP5P, and SPC/E water force fields, in a wide temperature and pressure range, limited however, within the supercritical region. The authors used 4,096 water molecules minimising thus the finite size effects. On the other hand, within the supercooled region, the extensive studies of Starr et al. [79], Mittal et al. [112], and Chopra et al. [395] were limited by the use of less than 1,000 SPC/E water molecules. In addition, the studies of Guevara-Carrion et al. [139] that used 2,048 TIP4P/2005 water molecules; Moulton et al. [173] that used 2,000 SPC/E, and TIP4P/2005 water molecules; and the study of Jiang et al. [190] that reported results using the HBP, BK3, and TIP4P/2005 water force fields, explore only a limited range of the $P - T$ plane of interest.

Therefore, to the best of our knowledge to this day, there is no specific molecular simulation study, using any water force field, that can satisfy simultaneously the following two criteria: (i) performed MD simulations of the water self-diffusivity at a wide T and P range, including the supercritical and the supercooled regions, and (ii) correctly accounting for system size effects by either incorporating corrections to the reported self-diffusivity values or by using a large number of water molecules (e.g. larger than 1,000). Consequently, the conclusions

regarding the performance of the examined water force fields, with respect to the self-diffusivity, need to be based on partial information. The discussion is further hampered by the lack of experimental measurements at various regions of interest that could be used for force field validations.

Nevertheless, based on the available information the following recommendations can be made regarding the computation of the water self-diffusivity. Six water force fields seem to be promising in providing reasonable predictions in a wide T and P range: Namely, the three polarisable force fields TIP4P-QDP-LJ, BK3, and HBP, the two-body, rigid TIP4P/2005, and flexible TIP4P/2005f, and the three-body E3B3. These force fields are good candidates for identifying the best model to consider in a future systematic study of the self-diffusivity of water. Among the issues that need to be discussed further, is the computational cost associated with using each one of the aforementioned force fields, considering the amount of computations that a systematic study would require.

Regarding the case of water in bulk, possible future contributions in the following research directions would be beneficial:

- Performing MD simulations with the most successful force fields, at high pressures, in order to verify if the self-diffusion coefficient exhibit maxima at isotherms (when $T < 315$ K).
- A systematic study for T 's in the supercooled region, including corrections for system size effects.
- Delineating the crossover temperature where the Stokes–Einstein theory is replaced by the fractional Stokes–Einstein and calculation of the fractional exponent, t . This effort would require the systematic study, using MD simulations, of the shear viscosity in addition to the self-diffusivity.
- Improve the performance of coarse-grained models regarding their ability to calculate accurately the water self-diffusivity in a wide T and P range.

On the other hand, regarding the case of water under confinement, possible future contributions in the following areas would be beneficial:

- The establishment of a methodology to accurately calculate the self-diffusion coefficient in confined media via MD, including an adequate theoretical framework to account for system size effects.
- A broader comparison between different force fields is still lacking, including the most successful ones for the bulk phase, to calculate confined water self-diffusion coefficient.

Acknowledgments

This publication was made possible by NPRP [grants number 6-1157-2-471, 6-1547-2-632, 8-1648-2-688] from the Qatar National Research Fund (a member of Qatar Foundation). The statements made herein are solely the responsibility of the authors. INT acknowledges partial support of the work by the project ‘Development of Materials and Devices for Industrial, Health, Environmental and Cultural Applications’ (MIS 5002567) which is implemented under the ‘Action for the Strategic Development on the Research and Technological Sector’, funded by the Operational Program ‘Competitiveness, Entrepreneurship and Innovation’ (NSRF 2014–2020) and co-financed by Greece and the European Union (European Regional Development Fund). OM and ME acknowledge

financial support from the department of Process & Energy, TU Delft. LFMF and MBMS acknowledge the financial support from CNPq (The Brazilian National Council for Scientific and Technological Development).

Disclosure statement

No potential conflict of interest was reported by the authors.

Funding

This work was supported by Qatar National Research Fund [grant number NPRP 6-1157-2-471, NPRP 6-1547-2-632, NPRP 8-1648-2-688]; partial support of the work by the project ‘Development of Materials and Devices for Industrial, Health, Environmental and Cultural Applications’ (MIS 5002567) which is implemented under the ‘Action for the Strategic Development on the Research and Technological Sector’, funded by the Operational Program ‘Competitiveness, Entrepreneurship and Innovation’ (NSRF 2014–2020) and co-financed by Greece and the European Union (European Regional Development Fund). OM and ME acknowledge financial support from the Department of Process & Energy, TU Delft. LFMF and MBMS acknowledge the financial support from CNPq (The Brazilian National Council for Scientific and Technological Development).

ORCID

Ioannis N. Tsimpanogiannis  <http://orcid.org/0000-0002-3466-1873>

Othonas A. Moulton  <http://orcid.org/0000-0001-7477-9684>

Luís F. M. Franco  <https://orcid.org/0000-0002-9334-9660>

Ioannis G. Economou  <http://orcid.org/0000-0002-2409-6831>

References

- [1] Bellissent-Funel MC, Hassanali A, Havenith M, et al. Water determines the structure and dynamics of proteins. *Chem Rev.* 2016;116:7673–7697.
- [2] Agmon N, Bakker HJ, Campen RK, et al. Protons and hydroxide ions in aqueous systems. *Chem Rev.* 2016;116:7642–7672.
- [3] Björneholm O, Hansen MH, Hodgson A, et al. Water at interfaces. *Chem Rev.* 2016;116:7698–7726.
- [4] Vega C, Abascal JLF. Simulating water with rigid non-polarizable models: a general perspective. *Phys Chem Chem Phys.* 2011;13:19663–19688.
- [5] Vega C. Water: one molecule, two surfaces, one mistake. *Mol Phys.* 2015;113:1145–1163.
- [6] Gallo P, Amann-Winkel K, Angell CA, et al. Water: a tale of two liquids. *Chem Rev.* 2016;116:7463–7500.
- [7] [cited 2018 May 21]. Available from: <http://www.lsbu.ac.uk/water/anmlies.html>.
- [8] Frenkel D, Smit B. Understanding molecular simulation: from algorithms to applications. 2nd ed. San Diego (CA): Academic Press; 2002.
- [9] Plimpton S. Fast parallel algorithms for short-range molecular dynamics. *J Comput Phys.* 1995;117:1–19.
- [10] Lindahl E, Hess B, van der Spoel D. GROMACS 3.0: a package for molecular simulation and trajectory analysis. *J Mol Model.* 2001;7:306–317.
- [11] Debenedetti PG, Stillinger Frank H. Supercooled liquids and the glass transition. *Nature.* 2001;410:259–267.
- [12] Stanley HE, Kumar P, Franzese G, et al. Liquid polyamorphism: possible relation to the anomalous behaviour of water. *Eur Phys J Spec Top.* 2008;161:1–17.
- [13] Stanley HE, Kumar P, Han S, et al. Heterogeneities in confined water and protein hydration water. *J Phys Condens Matter.* 2009;21:504105.
- [14] Stanley HE, Buldyrev SV, Franzese G, et al. Liquid polymorphism: water in nanoconfined and biological environments. *J Phys Condens Matter.* 2010;22:284101.

- [15] Bartels-Rausch T, Bergeron V, Cartwright JHE, et al. Ice structures, patterns, and processes: a view across the icefields. *Rev Mod Phys.* 2012;84:885–944.
- [16] Wallqvist A, Mountain RD. Molecular models of water: derivation and description. *Rev Comput Chem.* 2007;13:183–247.
- [17] Striolo A, Michaelides A, Joly L. The carbon-water interface: modeling challenges and opportunities for the water-energy nexus. *Annu Rev Chem Biomol Eng.* 2016;7:533–556.
- [18] Gillan MJ, Alfè D, Michaelides A. Perspective: how good is DFT for water? *J Chem Phys.* 2016;144:130901.
- [19] Cisneros GA, Wikfeldt KT, Ojamäe L, et al. Modeling molecular interactions in water: from pairwise to many-body potential energy functions. *Chem Rev.* 2016;116:7501–7528.
- [20] Ceriotti M, Fang W, Kusalik PG, et al. Nuclear quantum effects in water and aqueous systems: experiment, theory, and current challenges. *Chem Rev.* 2016;116:7529–7550.
- [21] Fransson T, Harada Y, Kosugi N, et al. X-ray and electron spectroscopy of water. *Chem Rev.* 2016;116:7551–7569.
- [22] Amann-Winkel K, Bellissent-Funel M-C, Bove LE, et al. X-ray and neutron scattering of water. *Chem Rev.* 2016;116:7570–7589.
- [23] Perakis F, De Marco L, Shalit A, et al. Vibrational spectroscopy and dynamics of water. *Chem Rev.* 2016;116:7590–7607.
- [24] Cervený S, Mallamace F, Swenson J, et al. Confined water as model of supercooled water. *Chem Rev.* 2016;116:7608–7625.
- [25] Liu H, Macedo EA. Accurate correlations for the self-diffusion coefficients of CO₂, CH₄, C₂H₄, H₂O, and D₂O over wide ranges of temperature and pressure. *J Supercrit Fluids.* 1995;8:310–317.
- [26] Krishna R, Van Baten JM. The darken relation for multicomponent diffusion in liquid mixtures of linear alkanes: an investigation using molecular dynamics (MD) simulations. *Ind Eng Chem Res.* 2005;44:6939–6947.
- [27] Rahman A, Stillinger FH. Molecular dynamics study of liquid water. *J Chem Phys.* 1971;55:3336–3359.
- [28] Stillinger FH, Rahman A. Improved simulation of liquid water by molecular dynamics. *J Chem Phys.* 1974;60:1545–1557.
- [29] Rahman A, Stillinger FH, Lemberg HL. Study of a central force model for liquid water by molecular dynamics. *J Chem Phys.* 1975;63:5223–5230.
- [30] Stillinger FH, Rahman A. Revised central force potentials for water. *J Chem Phys.* 1978;68:666–670.
- [31] Impey RW, Madden PA, McDonald IR. Spectroscopic and transport properties of water. *Mol Phys.* 1982;46:513–539.
- [32] Jorgensen WL, Chandrasekhar J, Madura JD, et al. Comparison of simple potential functions for simulating liquid water. *J Chem Phys.* 1983;79:926–935.
- [33] Jancsó G, Bopp P, Heinzinger K. Molecular dynamics study of high-density liquid water using a modified central-force potential. *Chem Phys.* 1984;85:377–387.
- [34] Ferrario M, Tani A. A molecular dynamics study of the TIP4P model of water. *Chem Phys Lett.* 1985;121:182–186.
- [35] Lie G, Clementi E. Molecular-dynamics simulation of liquid water with an *ab initio* flexible water-water interaction potential. *Phys Rev A.* 1986;33:2679–2693.
- [36] Neumann M. Dielectric relaxation in water. Computer simulations with the TIP4P potential. *J Chem Phys.* 1986;85:1567–1580.
- [37] Wojcik M, Clementi E. Single molecule dynamics of three body water. *J Chem Phys.* 1986;85:3544–3549.
- [38] Anderson J, Ullo J, Yip S. Molecular dynamics simulation of dielectric properties of water. *J Chem Phys.* 1987;87:1726–1732.
- [39] Berendsen HJC, Grigera JR, Straatsma TP. The missing term in effective pair potentials. *J Phys Chem.* 1987;91:6269–6271.
- [40] Reddy MR, Berkowitz M. Structure and dynamics of high-pressure TIP4P water. *J Chem Phys.* 1987;87:6682–6686.
- [41] Teleman O, Jönsson B, Engström S. A molecular dynamics simulation of a water model with intramolecular degrees of freedom. *Mol Phys.* 1987;60:193–203.
- [42] Ahlström P, Wallqvist A, Engström S, et al. A molecular dynamics study of polarizable water. *Mol Phys.* 1989;68:563–581.
- [43] Watanabe K, Klein ML. Effective pair potentials and the properties of water. *Chem Phys.* 1989;131:157–167.
- [44] Caldwell J, Kollman PA, Dang LX. Implementation of nonadditive intermolecular potentials by use of molecular dynamics: development of a water-water potential and water-ion cluster interactions. *J Am Chem Soc.* 1990;112:9144–9147.
- [45] Wallqvist A, Ahlstrom P, Karlstroms G. A new intermolecular energy calculation scheme: applications to potential surface and liquid properties of water. *J Phys Chem.* 1990;94:1649–1656.
- [46] Ruff I, Diestler DJ. Isothermal-isobaric molecular dynamics simulation of liquid water. *J Chem Phys.* 1990;93:2032–2042.
- [47] Sprik M, Klein ML, Watanabe K. Solvent polarization and hydration of the chlorine anion. *J Phys Chem.* 1990;94:6483–6488.
- [48] Straatsma TP, McCammon JA. Molecular dynamics simulations with interaction potentials including polarization development of a noniterative method and application to water. *Mol Simul.* 1990;5:181–192.
- [49] Barrat JL, McDonald IR. The role of molecular flexibility in simulations of water. *Mol Phys.* 1990;70:535–539.
- [50] Brodholt J, Wood B. Molecular dynamics of water at high temperatures and pressures. *Geochim Cosmochim Acta.* 1990;54:2611–2616.
- [51] Frattini R, Ricci MA, Ruocco G, et al. Temperature evolution of single particle correlation functions of liquid water. *J Chem Phys.* 1990;92:2540–2547.
- [52] Sprik M. Hydrogen bonding and the static dielectric constant in liquid water. *J Chem Phys.* 1991;95:6762–6769.
- [53] Zhu S, Singh S, Robinson GW, et al. A new flexible/polarizable water model. *J Chem Phys.* 1991;95:2791–2799.
- [54] Zhu SB, Yao S, Zhu JB, et al. A flexible/polarizable simple point charge water model. *J Phys Chem.* 1991;95:6211–6217.
- [55] Wallqvist A, Teleman O. Properties of flexible water models. *Mol Phys.* 1991;74:515–533.
- [56] Smith DE, Haymet ADJ. Structure and dynamics of water and aqueous solutions: the role of flexibility. *J Chem Phys.* 1992;96:8450–8459.
- [57] Van Belle D, Froeyen M, Lippens G, et al. Molecular dynamics simulation of polarizable water by an extended lagrangian method. *Mol Phys.* 1992;77:239–255.
- [58] Sciortino F, Geiger A, Stanley HE. Network defects and molecular mobility in liquid water. *J Chem Phys.* 1992;96:3857–3865.
- [59] Guissani Y, Guillot B. A computer simulation study of the liquid-vapor coexistence curve of water. *J Chem Phys.* 1993;98:8221–8235.
- [60] Rick SW, Stuart SJ, Berne BJ. Dynamical fluctuating charge force fields: application to liquid water. *J Chem Phys.* 1994;101:6141–6156.
- [61] Smith DE, Dang LX. Computer simulations of NaCl association in polarizable water. *J Chem Phys.* 1994;100:3757–3766.
- [62] Svishchev IM, Kusalik P. Dynamics in liquid H₂O, D₂O, and T₂O: a comparative simulation study. *J Phys Chem.* 1994;98:728–733.
- [63] Padro JA, Marti J, Guardia E. Molecular dynamics simulation of liquid water at 523K. *J Phys Condens Matt.* 1994;6:2283–2290.
- [64] Báez LA, Clancy P. Existence of a density maximum in extended simple point charge water. *J Chem Phys.* 1994;101:9837–9840.
- [65] Åstrand PO, Linse P, Karlström G. Molecular dynamics study of water adopting a potential function with explicit atomic dipole moments and anisotropic polarizabilities. *Chem Phys.* 1995;191:195–202.
- [66] Soetens JC, Millot C. Effect of distributing multipoles and polarizabilities on molecular dynamics simulations of water. *Chem Phys Lett.* 1995;235:22–30.
- [67] Duan Z, Møller N, Weare JH. Molecular dynamics simulation of water properties using RWK2 potential: from clusters to bulk water. *Geochim Cosmochim Acta.* 1995;59:3273–3283.
- [68] Mountain RD. Comparison of a fixed-charge and a polarizable water model. *J Chem Phys.* 1995;103:3084–3090.
- [69] Brodholt J, Sampoli M, Vallauri R. Parameterizing a polarizable intermolecular potential for water. *Mol Phys.* 1995;86:149–158.
- [70] Svishchev IM, Kusalik PG, Wang J, et al. Polarizable point-charge model for water: results under normal and extreme conditions. *J Chem Phys.* 1996;105:4742–4750.

- [71] Gallo P, Sciortino F, Tartaglia P, et al. Slow dynamics of water molecules in supercooled states. *Phys Rev Lett*. 1996;76:2730–2733.
- [72] Sciortino F, Gallo P, Tartaglia P, et al. Supercooled water and the kinetic glass transition. *Phys Rev E*. 1996;54:6331–6343.
- [73] Taylor RS, Dang LX, Garrett BC. Molecular dynamics simulations of the liquid/vapor interface of SPC/E water. *J Phys Chem*. 1996;100:11720–11725.
- [74] Bagchi K, Balasubramanian S, Klein ML. The effects of pressure on structural and dynamical properties of associated liquids: molecular dynamics calculations for the extended simple point charge model of water. *J Chem Phys*. 1997;107:8561–8567.
- [75] Dang LX, Chang TM. Molecular dynamics study of water clusters, liquid, and liquid-vapor interface of water with many-body potentials. *J Chem Phys*. 1997;106:8149–8159.
- [76] Levitt M, Hirshberg M, Sharon R, et al. Calibration and testing of a water model for simulation of the molecular dynamics of proteins and nucleic acids in solution. *J Phys Chem B*. 1997;101:5051–5061.
- [77] Lobaugh J, Voth GA. A quantum model for water: equilibrium and dynamical properties. *J Chem Phys*. 1997;106:2400–2410.
- [78] de Leeuw N, Parker S. Molecular-dynamics simulation of MgO surfaces in liquid water using a shell-model potential for water. *Phys Rev B*. 1998;58:13901–13908.
- [79] Starr FW, Sciortino F, Stanley HE. Dynamics of simulated water under pressure. *Phys Rev B*. 1999;60:6757–6768.
- [80] Svishchev IM, Zassetsky AY. Self-diffusion process in water: spatial picture of single-particle density fluctuations. *J Chem Phys*. 2000;113:7432–7436.
- [81] Nymand TM, Linse P. Molecular dynamics simulations of polarizable water at different boundary conditions. *J Chem Phys*. 2000;112:6386–6395.
- [82] Guo G-J, Zhang Y-G. Equilibrium molecular dynamics calculation of the bulk viscosity of liquid water. *Mol Phys*. 2001;99:283–289.
- [83] Mahoney MW, Jorgensen WL. Diffusion constant of the TIP5P model of liquid water. *J Chem Phys*. 2001;114:363–366.
- [84] Stern HA, Rittner F, Berne BJ, et al. Combined fluctuating charge and polarizable dipole models: application to a five-site water potential function. *J Chem Phys*. 2001;115:2237–2251.
- [85] van Maaren PJ, van der Spoel D. Molecular dynamics simulations of water with novel shell-model potentials. *J Phys Chem B*. 2001;105:2618–2626.
- [86] Lefohn AE, Ovchinnikov M, Voth GA. A multistate empirical valence bond approach to a polarizable and flexible water model. *J Phys Chem B*. 2001;105:6628–6637.
- [87] Guillot B, Guissani Y. How to build a better pair potential for water. *J Chem Phys*. 2001;114:6720–6733.
- [88] Errington J, Debenedetti P. Relationship between structural order and the anomalies of liquid water. *Nature*. 2001;409:318–321.
- [89] Burnham CJ, Xantheas SS. Development of transferable interaction models for water. III. reparametrization of an all-atom polarizable rigid model (TTM2-R) from first principles. *J Chem Phys*. 2002;116:1500–1510.
- [90] Guo G-J, Zhang Y-G, Refson K, et al. Viscosity and stress autocorrelation function in supercooled water: a molecular dynamics study. *Mol Phys*. 2002;100:2617–2627.
- [91] English NJ, MacElroy JMD. Atomistic simulations of liquid water using Lekner electrostatics. *Mol Phys*. 2002;100:3753–3769.
- [92] Nieto-Draghi C, Bonet Avalos J, Rousseau B. Dynamic and structural behavior of different rigid nonpolarizable models of water. *J Chem Phys*. 2003;118:7954–7964.
- [93] Yamaguchi T, Chong S-H, Hirata F. Theoretical study of the molecular motion of liquid water under high pressure. *J Chem Phys*. 2003;119:1021–1034.
- [94] Tan ML, Fischer JT, Chandra A, et al. A temperature of maximum density in soft sticky dipole water. *Chem Phys Lett*. 2003;376:646–652.
- [95] Yu H, Hansson T, van Gunsteren WF. Development of a simple, self-consistent polarizable model for liquid water. *J Chem Phys*. 2003;118:221–234.
- [96] Jeon J, Lefohn AE, Voth GA. An improved polarflex water model. *J Chem Phys*. 2003;118:7504–7518.
- [97] English NJ, MacElroy JMD. Hydrogen bonding and molecular mobility in liquid water in external electromagnetic fields. *J Chem Phys*. 2003;119:11806–11813.
- [98] Ren P, Ponder JW. Polarizable atomic multipole water model for molecular mechanics simulation. *J Phys Chem B*. 2003;107:5933–5947.
- [99] Spångberg D, Hermansson K. Effective three-body potentials for Li^+ (aq) and Mg^{2+} (aq). *J Chem Phys*. 2003;119:7263–7281.
- [100] Amira S, Spångberg D, Hermansson K. Derivation and evaluation of a flexible SPC model for liquid water. *Chem Phys*. 2004;303:327–334.
- [101] Horn HW, Swope WC, Pitera JW, et al. Development of an improved four-site water model for biomolecular simulations: TIP4P-Ew. *J Chem Phys*. 2004;120:9665–9678.
- [102] Yeh IC, Hummer G. System-size dependence of diffusion coefficients and viscosities from molecular dynamics simulations with periodic boundary conditions. *J Phys Chem B*. 2004;108:15873–15879.
- [103] Ren P, Ponder JW. Temperature and pressure dependence of the AMOEBA water model. *J Phys Chem B*. 2004;108:13427–13437.
- [104] Saint-Martin H, Hernández-Cobos J, Ortega-Blake I. Water models based on a single potential energy surface and different molecular degrees of freedom. *J Chem Phys*. 2005;122:224509.
- [105] Abascal JLF, Vega C. A general purpose model for the condensed phases of water: TIP4P/2005. *J Chem Phys*. 2005;123:234505.
- [106] Xu L, Kumar P, Buldyrev SV, et al. Relation between the Widom line and the dynamic crossover in systems with a liquid–liquid phase transition. *Proc Natl Acad Sci USA*. 2005;102:16558–16562.
- [107] Lamoureux G, Harder E, Vorobyov I, et al. A polarizable model of water for molecular dynamics simulations of biomolecules. *Chem Phys Lett*. 2006;418:245–249.
- [108] Wu Y, Tepper HL, Voth GA. Flexible simple point-charge water model with improved liquid-state properties. *J Chem Phys*. 2006;124:024503.
- [109] Paesani F, Zhang W, Case DA, et al. An accurate and simple quantum model for liquid water. *J Chem Phys*. 2006;125:184507.
- [110] Fanourgakis GS, Xantheas SS. The flexible, polarizable, Thole-type interaction potential for water (TTM2-F) revisited. *J Phys Chem A*. 2006;110:4100–4106.
- [111] Donchev AG, Galkin NG, Illarionov AA, et al. Water properties from first principles: simulations by a general-purpose quantum mechanical polarizable force field. *Proc Natl Acad Sci USA*. 2006;103:8613–8617.
- [112] Mittal J, Errington JR, Truskett TM. Quantitative link between single-particle dynamics and static structure of supercooled liquids. *J Phys Chem B*. 2006;110:18147–18150.
- [113] Yoshida K, Matubayasi N, Nakahara M. Self-diffusion of supercritical water in extremely low-density region. *J Chem Phys*. 2006;125:074307.
- [114] Hofmann DWM, Kuleshova L, D’Aguanno B. A new reactive potential for the molecular dynamics simulation of liquid water. *Chem Phys Lett*. 2007;448:138–143.
- [115] Defusco A, Schofield DP, Jordan KD. Comparison of models with distributed polarizable sites for describing water clusters. *Mol Phys*. 2007;105:2681–2696.
- [116] Yoshida K, Matubayasi N, Nakahara M. Solvation shell dynamics studied by molecular dynamics simulation in relation to the translational and rotational dynamics of supercritical water and benzene. *J Chem Phys*. 2007;127:174509.
- [117] Kumar P, Buldyrev SV, Becker SR, et al. Relation between the Widom line and the breakdown of the Stokes-Einstein relation in supercooled water. *Proc Natl Acad Sci USA*. 2007;104:9575–9579.
- [118] Kolafa J. A polarizable three-site water model with intramolecular polarizability. *Collect Czechoslov Chem Commun*. 2008;73:507–517.
- [119] Mankoo PK, Keyes T. POLIR: polarizable, flexible, transferable water potential optimized for IR spectroscopy. *J Chem Phys*. 2008;129:034504.
- [120] Liem SY, Popelier PLA. Properties and 3D structure of liquid water: a perspective from a high-rank multipolar electrostatic potential. *J Chem Theory Comput*. 2008;4:353–365.

- [121] Kumar R, Skinner JL. Water simulation model with explicit three-molecule interactions. *J Phys Chem B*. 2008;112:8311–8318.
- [122] Akin-Ojo O, Song Y, Wang F. Developing *ab initio* quality force fields from condensed phase quantum-mechanics/molecular-mechanics calculations through the adaptive force matching method. *J Chem Phys*. 2008;129:064108.
- [123] Vega C, Abascal JLF, Conde MM, et al. What ice can teach us about water interactions: a critical comparison of the performance of different water models. *Faraday Discuss*. 2009;141:251–276.
- [124] Walsh TR, Liang T. A multipole-based water potential with implicit polarization for biomolecular simulations. *J Comput Chem*. 2009;30:893–899.
- [125] Bauer BA, Warren GL, Patel S. Incorporating phase-dependent polarizability in nonadditive electrostatic models for molecular dynamics simulations of the aqueous liquid vapor interface. *J Chem Theory Comput*. 2009;5:359–373.
- [126] Bauer BA, Patel S. Properties of water along the liquid-vapor coexistence curve via molecular dynamics simulations using the polarizable TIP4P-QDP-LJ water model. *J Chem Phys*. 2009;131:084709.
- [127] Liu J, Miller WH, Paesani F, et al. Quantum dynamical effects in liquid water: a semiclassical study on the diffusion and the infrared absorption spectrum. *J Chem Phys*. 2009;131:164509.
- [128] Kunz A-PE, van Gunsteren WF. Development of a nonlinear classical polarization model for liquid water and aqueous solutions: COS/D. *J Phys Chem A*. 2009;113:11570–11579.
- [129] Akin-Ojo O, Wang F. Improving the point-charge description of hydrogen bonds by adaptive force matching. *J Phys Chem B*. 2009;113:1237–1240.
- [130] Molinero V, Moore EB. Water modeled as an intermediate element between carbon and silicon. *J Phys Chem B*. 2009;113:4008–4016.
- [131] Pi HL, Aragonés JL, Vega C, et al. Anomalies in water as obtained from computer simulations of the TIP4P/2005 model: density maxima, and density, isothermal compressibility and heat capacity minima. *Mol Phys*. 2009;107:365–374.
- [132] Te JA, Ichiye T. Temperature and pressure dependence of the optimized soft-sticky dipole-quadrupole-octupole water model. *J Chem Phys*. 2010;132:114511.
- [133] Shaik MS, Liem SY, Popelier PLA. Properties of liquid water from a systematic refinement of a high-rank multipolar electrostatic potential. *J Chem Phys*. 2010;132:174504.
- [134] Chiu S, Scott HL, Jakobsson E. A coarse-grained model based on morse potential for water and *n*-alkanes. *J Chem Theory Comput*. 2010;6:851–863.
- [135] Karamertzanis PG, Raiteri P, Galindo A. The use of anisotropic potentials in modeling water and free energies of hydration. *J Chem Theory Comput*. 2010;6:1590–1607.
- [136] Darre L, Machado MR, Dans PD, et al. Another coarse grain model for aqueous solvation: WAT FOUR? *J Chem Theory Comput*. 2010;6:3793–3807.
- [137] Fuhrmans M, Sanders BP, Marrink SJ, et al. Effects of bundling on the properties of the SPC water model. *Theor Chem Acc*. 2010;125:335–344.
- [138] Chopra R, Truskett TM, Errington JR. On the use of excess entropy scaling to describe single-molecule and collective dynamic properties of hydrocarbon isomer fluids. *J Phys Chem B*. 2010;114:16487–16493.
- [139] Guevara-Carrion G, Vrabec J, Hasse H. Prediction of self-diffusion coefficient and shear viscosity of water and its binary mixtures with methanol and ethanol by molecular simulation. *J Chem Phys*. 2011;134:074508.
- [140] Tainter CJ, Pieniazek PA, Lin YS, et al. Robust three-body water simulation model. *J Chem Phys*. 2011;134:184501.
- [141] González MA, Abascal JLF. A flexible model for water based on TIP4P/2005. *J Chem Phys*. 2011;135:224516.
- [142] Hasegawa T, Tanimura Y. A polarizable water model for intramolecular and intermolecular vibrational spectroscopies. *J Phys Chem B*. 2011;115:5545–5553.
- [143] Alexandre J, Chapela GA, Saint-Martin H, et al. A non-polarizable model of water that yields the dielectric constant and the density anomalies of the liquid: TIP4Q. *Phys Chem Chem Phys*. 2011;13:19728–19740.
- [144] Viererblová L, Kolafa J. A classical polarizable model for simulations of water and ice. *Phys Chem Chem Phys*. 2011;13:19925–19935.
- [145] Orsi M, Essex JW. The ELBA force field for coarse-grain modeling of lipid membranes. *PLoS One*. 2011;6:e28637.
- [146] Wang J, Hou T. Application of molecular dynamics simulations in molecular property prediction II: diffusion coefficient. *J Comput Chem*. 2011;32:3505–3519.
- [147] Qvist J, Schober H, Halle B. Structural dynamics of supercooled water from quasielastic neutron scattering and molecular simulations. *J Chem Phys*. 2011;134:144508.
- [148] Raabe G, Sadus RJ. Molecular dynamics simulation of the effect of bond flexibility on the transport properties of water. *J Chem Phys*. 2012;137:104512.
- [149] Leontyev I V, Stuchebrukhov AA. Polarizable mean-field model of water for biological simulations with AMBER and CHARMM force fields. *J Chem Theory Comput*. 2012;8:3207–3216.
- [150] Darré L, Tek A, Baaden M, et al. Mixing atomistic and coarse grain solvation models for MD simulations: let WT4 handle the bulk. *J Chem Theory Comput*. 2012;8:3880–3894.
- [151] Babin V, Medders GR, Paesani F. Toward a universal water model: first principles simulations from the dimer to the liquid phase. *J Phys Chem Lett*. 2012;3:3765–3769.
- [152] Tazi S, Boan A, Salanne M, et al. Diffusion coefficient and shear viscosity of rigid water models. *J Phys Condens Matter*. 2012;24:284117.
- [153] Gallo P, Rovere M. Mode coupling and fragile to strong transition in supercooled TIP4P water. *J Chem Phys*. 2012;137:164503.
- [154] Rozmanov D, Kusalik PG. Transport coefficients of the TIP4P-2005 water model. *J Chem Phys*. 2012;136:044507.
- [155] Zlenko D V. Computing the self-diffusion coefficient for TIP4P water. *Biophysics (Oxf)*. 2012;57:127–132.
- [156] Lee SH. Temperature dependence on structure and self-diffusion of water: a molecular dynamics simulation study using SPC/E model. *Bull Korean Chem Soc*. 2013;34:3800–3804.
- [157] Chen Y, Li AH, Wang Y, et al. Molecular dynamics simulations of liquid water structure and diffusivity. *Chinese J Phys*. 2013;51:1218–1229.
- [158] Akin-Ojo O, Szalewicz K. How well can polarization models of pairwise nonadditive forces describe liquid water? *J Chem Phys*. 2013;138:024316.
- [159] Yu W, Lopes PEM, Roux B, et al. Six-site polarizable model of water based on the classical drude oscillator. *J Chem Phys*. 2013;138:034508.
- [160] Kiss PT, Baranyai A. A systematic development of a polarizable potential of water. *J Chem Phys*. 2013;138:204507.
- [161] Corsetti F, Artacho E, Soler JM, et al. Room temperature compressibility and diffusivity of liquid water from first principles. *J Chem Phys*. 2013;139:194502.
- [162] Han J, Mazack MJM, Zhang P, et al. Quantum mechanical force field for water with explicit electronic polarization. *J Chem Phys*. 2013;139:054503.
- [163] Baker CM, Best RB. Matching of additive and polarizable force fields for multiscale condensed phase simulations. *J Chem Theory Comput*. 2013;9:2826–2837.
- [164] Nagarajan A, Junghans C, Matysiak S. Multiscale simulation of liquid water using a four-to-one mapping for coarse-graining. *J Chem Theory Comput*. 2013;9:5168–5175.
- [165] Stukan MR, Asmadi A, Abdallah W. Bulk properties of SWM4-NDP water model at elevated temperature and pressure. *J Mol Liq*. 2013;180:65–69.
- [166] Tröster P, Lorenzen K, Schwörer M, et al. Polarizable water models from mixed computational and empirical optimization. *J Phys Chem B*. 2013;117:9486–9500.
- [167] Wang L-P, Head-Gordon T, Ponder JW, et al. Systematic improvement of a classical molecular model of water. *J Phys Chem B*. 2013;117:9956–9972.
- [168] Arismendi-Arrieta D, Medina JS, Fanourgakis GS, et al. Simulating liquid water for determining its structural and transport properties. *Appl Radiat Isot*. 2014;83:115–121.

- [169] Braun D, Boresch S, Steinhauser O. Transport and dielectric properties of water and the influence of coarse-graining: transport and dielectric properties of water and the influence of coarse-graining: comparing BMW, SPC/E, and TIP3P models. *J Chem Phys.* 2014;140:064107.
- [170] Bachmann SJ, Van Gunsteren WF. An improved simple polarisable water model for use in biomolecular simulation. *J Chem Phys.* 2014;141:22D515.
- [171] Fuentes-Azcatl R, Alejandre J. Non-polarizable force field of water based on the dielectric constant: TIP4P/ε. *J Phys Chem B.* 2014;118:1263–1272.
- [172] Tröster P, Lorenzen K, Tavan P. Polarizable six-point water models from computational and empirical optimization. *J Phys Chem B.* 2014;118:1589–1602.
- [173] Moulτος OA, Tsimpanogiannis IN, Panagiotopoulos AZ, et al. Atomistic molecular dynamics simulations of CO₂ diffusivity in H₂O for a wide range of temperatures and pressures. *J Phys Chem B.* 2014;118:5532–5541.
- [174] Izadi S, Anandakrishnan R, Onufriev A V. Building water models: a different approach. *J Phys Chem Lett.* 2014;5:3863–3871.
- [175] Spura T, John C, Habershon S, et al. Nuclear quantum effects in liquid water from path-integral simulations using an *ab initio* force-matching approach. *Mol Phys.* 2015;113:808–822.
- [176] Orsi M. Comparative assessment of the ELBA coarse-grained model for water. *Mol Phys.* 2014;112:1566–1576.
- [177] Bachmann SJ, Van Gunsteren WF. On the compatibility of polarisable and non-polarisable models for liquid water. *Mol Phys.* 2014;112:2761–2780.
- [178] Medders GR, Babin V, Paesani F. Development of a “first-principles” water potential with flexible monomers. III. Liquid phase properties. *J Chem Theory Comput.* 2014;10:2906–2910.
- [179] Kiss PT, Baranyai A. Anomalous properties of water predicted by the BK3 model. *J Chem Phys.* 2014;140:154505.
- [180] Espinosa JR, Sanz E, Valeriani C, et al. Homogeneous ice nucleation evaluated for several water models. *J Chem Phys.* 2014;141:18C529.
- [181] Shvab I, Sadus RJ. Thermodynamic properties and diffusion of water + methane binary mixtures. *J Chem Phys.* 2014;140:104505.
- [182] Gallo P, Corradini D, Rovere M. Widom line and dynamical crossovers as routes to understand supercritical water. *Nat Commun.* 2014;5:5806.
- [183] Tainter CJ, Shi L, Skinner JL. Reparametrized E3B (explicit three-body) water model using the TIP4P/2005 model as a reference. *J Chem Theory Comput.* 2015;11:2268–2277.
- [184] Lobanova O, Avendaño C, Lafitte T, et al. SAFT-γ force field for the simulation of molecular fluids: 4. A single-site coarse-grained model of water applicable over a wide temperature range. *Mol Phys.* 2015;113:1228–1249.
- [185] Park DK, Yoon B-W, Lee SH. Transport properties of super-cooled water: a molecular dynamics simulation study using SPC/E model. *Bull Korean Chem Soc.* 2015;36:492–497.
- [186] Fuentes-Azcatl R, Mendoza N, Alejandre J. Improved SPC force field of water based on the dielectric constant: SPC/ε. *Phys A Stat Mech its Appl.* 2015;420:116–123.
- [187] Shvab I, Sadus RJ. Thermophysical properties of supercritical water and bond flexibility. *Phys Rev E.* 2015;92:012124.
- [188] Corradini D, Rovere M, Gallo P. The Widom line and dynamical crossover in supercritical water: popular water models versus experiments. *J Chem Phys.* 2015;143:114502.
- [189] Tran KN, Tan M, Ichiye T. A single-site multipole model for liquid water. *J Chem Phys.* 2016;145:034501.
- [190] Jiang H, Moulτος OA, Economou IG, et al. Hydrogen-bonding polarizable intermolecular potential model for water. *J Phys Chem B.* 2016;120:12358–12370.
- [191] Ding W, Palaiokostas M, Orsi M. Stress testing the ELBA water model. *Mol Simul.* 2016;42:337–346.
- [192] Köster A, Spura T, Rutkai G, et al. Assessing the accuracy of improved force-matched water models derived from *ab initio* molecular dynamics simulations. *J Comput Chem.* 2016;37:1828–1838.
- [193] Dhabal D, Chakravarty C, Molinero V, et al. Comparison of liquid-state anomalies in stillinger-weber models of water, silicon, and germanium. *J Chem Phys.* 2016;145:214502.
- [194] Guillaud E, Merabia S, de Ligny D, et al. Decoupling of viscosity and relaxation processes in supercooled water: a molecular dynamics study with the TIP4P/2005f model. *Phys Chem Chem Phys.* 2017;19:2124–2130.
- [195] Abbaspour M, Akbarzadeh H, Salemi S, et al. Molecular dynamics simulation of liquid water and ice nanoclusters using a new effective HFD-like model. *J Comput Chem.* 2018;39:269–278.
- [196] Gabrieli A, Sant M, Izadi S, et al. High-temperature dynamic behavior in bulk liquid water: a molecular dynamics simulation study using the OPC and TIP4P-Ew potentials. *Front Phys.* 2018;13:138203–138215.
- [197] Handle PH, Sciortino F. The Adam – Gibbs relation and the TIP4P/2005 model of water. *Mol Phys.* 2018;In press.
- [198] Striolo A. The mechanism of water diffusion in narrow carbon nanotubes. *Nano Lett.* 2006;6:633–639.
- [199] Striolo A. Water self-diffusion through narrow oxygenated carbon nanotubes. *Nanotechnology.* 2007;18:475704.
- [200] Nie GX, Wang Y, Huang JP. Shape effect of nanochannels on water mobility. *Front Phys.* 2016;11:114702.
- [201] Zheng Y, Ye H, Zhang Z, et al. Water diffusion inside carbon nanotubes: mutual effects of surface and confinement. *Phys Chem Chem Phys.* 2012;14:964–971.
- [202] Chiavazzo E, Fasano M, Asinari P, et al. Scaling behaviour for the water transport in nanoconfined geometries. *Nat Commun.* 2014;5:3565.
- [203] Martí J, Gordillo MC. Microscopic dynamics of confined supercritical water. *Chem Phys Lett.* 2002;354:227–232.
- [204] Barati Farimani A, Aluru NR. Spatial diffusion of water in carbon nanotubes: from fickian to ballistic motion. *J Phys Chem B.* 2011;115:12145–12149.
- [205] Liu Y, Wang Q. Transport behavior of water confined in carbon nanotubes. *Phys Rev B.* 2005;72:085420.
- [206] Hirunsit P, Balbuena PB. Effects of confinement on water structure and dynamics: a molecular simulation study. *J Phys Chem C.* 2007;111:1709–1715.
- [207] Sanghi T, Aluru NR. A combined quasi-continuum/Langevin equation approach to study the self-diffusion dynamics of confined fluids. *J Chem Phys.* 2013;138:124109.
- [208] Mozaffari F. A molecular dynamics simulation study of the effect of water–graphene interaction on the properties of confined water. *Mol Simul.* 2016;42:1475–1484.
- [209] Muscatello J, Jaeger F, Matar OK, et al. Optimizing water transport through graphene-based membranes: insights from nonequilibrium molecular dynamics. *ACS Appl Mater Interfaces.* 2016;8:12330–12336.
- [210] Sendner C, Horinek D, Bocquet L, et al. Interfacial water at hydrophobic and hydrophilic surfaces: slip, viscosity, and diffusion. *Langmuir.* 2009;25:10768–10781.
- [211] Nguyen TX, Bhatia SK. Some anomalies in the self-diffusion of water in disordered carbons. *J Phys Chem C.* 2012;116:3667–3676.
- [212] Diallo SO, Vlcek L, Mamontov E, et al. Translational diffusion of water inside hydrophobic carbon micropores studied by neutron spectroscopy and molecular dynamics simulation. *Phys Rev E.* 2015;91:022124.
- [213] Gordillo MC, Martí J. High temperature behavior of water inside flat graphite nanochannels. *Phys Rev B.* 2007;75:085406.
- [214] Martí J, Sala J, Guàrdia E. Molecular dynamics simulations of water confined in graphene nanochannels: from ambient to supercritical environments. *J Mol Liq.* 2010;153:72–78.
- [215] Martí J, Sala J, Guàrdia E, et al. Molecular dynamics simulations of supercritical water confined within a carbon-slit pore. *Phys Rev E.* 2009;79:031606.
- [216] Tahat A, Martí J. Proton transfer in liquid water confined inside graphene slabs. *Phys Rev E – Stat Nonlinear, Soft Matter Phys.* 2015;92:032402.
- [217] Martí J, Nagy G, Guàrdia E, et al. Molecular dynamics simulation of liquid water confined inside graphite channels: dielectric and dynamical properties. *J Phys Chem B.* 2006;110:23987–23994.

- [218] Mosaddeghi H, Alavi S, Kowsari MH, et al. Simulations of structural and dynamic anisotropy in nano-confined water between parallel graphite plates. *J Chem Phys.* 2012;137:184703.
- [219] Spera MBM, Taketa TB, Beppu MM. Roughness dynamic in surface growth: layer-by-layer thin films of carboxymethyl cellulose/chitosan for biomedical applications. *Biointerphases.* 2017;12:04E401.
- [220] Wei MJ, Zhou J, Lu X, et al. Diffusion of water molecules confined in slits of rutile TiO₂(110) and graphite(0001). *Fluid Phase Equilib.* 2011;302:316–320.
- [221] Choudhury N, Pettitt BM. Dynamics of water trapped between hydrophobic solutes. *J Phys Chem B.* 2005;109:6422–6429.
- [222] Kim JS, Choi JS, Lee MJ, et al. Between scylla and charybdis: hydrophobic graphene-guided water diffusion on hydrophilic substrates. *Sci Rep.* 2013;3:2309.
- [223] Spohr E, Hartnig C, Gallo P, et al. Water in porous glasses. A computer simulation study. *J Mol Liq.* 1999;80:165–178.
- [224] Leng Y, Cummings PT. Hydration structure of water confined between mica surfaces. *J Chem Phys.* 2006;124:1–5.
- [225] Porion P, Michot LJ, Faugère AM, et al. Structural and dynamical properties of the water molecules confined in dense clay sediments: a study combining 2H NMR spectroscopy and multiscale numerical modeling. *J Phys Chem C.* 2007;111:5441–5453.
- [226] Ou X, Li J, Lin Z. Dynamic behavior of interfacial water on Mg(OH)₂ (001) surface: a molecular dynamics simulation work. *J Phys Chem C.* 2014;118:29887–29895.
- [227] De Li T, Gao J, Szoszkiewicz R, et al. Structured and viscous water in subnanometer gaps. *Phys Rev B.* 2007;75:115415.
- [228] Kerisit S, Liu C. Molecular simulations of water and ion diffusion in nanosized mineral fractures. *Env Sci Technol.* 2009;43:777–782.
- [229] Mutisya SM, Kirch A, De Almeida JM, et al. Molecular dynamics simulations of water confined in calcite slit pores: an NMR spin relaxation and hydrogen bond analysis. *J Phys Chem C.* 2017;121:6674–6684.
- [230] Liu P, Harder E, Berne BJ. On the calculation of diffusion coefficients in confined fluids and interfaces with an application to the liquid-vapor interface of water. *J Phys Chem B.* 2004;108:6595–6602.
- [231] Prakash M, Lemaire T, Caruel M, et al. Anisotropic diffusion of water molecules in hydroxyapatite nanopores. *Phys Chem Miner.* 2017;44:509–519.
- [232] Prakash M, Lemaire T, Di Tommaso D, et al. Transport properties of water molecules confined between hydroxyapatite surfaces: a molecular dynamics simulation approach. *Appl Surf Sci.* 2017;418:296–301.
- [233] Pham TT, Lemaire T, Capiez-Lernout E, et al. Properties of water confined in hydroxyapatite nanopores as derived from molecular dynamics simulations. *Theor Chem Acc.* 2015;134:1.
- [234] Předota M, Cummings PT, Wesolowski DJ. Electric double layer at the rutile (110) surface. 3. Inhomogeneous viscosity and diffusivity measurement by computer simulations. *J Phys Chem C.* 2007;111:3071–3079.
- [235] Solveyra EG, de la Llave E, Molinero V, et al. Structure, dynamics, and phase behavior of water in TiO₂ nanopores. *J Phys Chem C.* 2013;117:3330–3342.
- [236] Cao W, Lu L, Huang L, et al. Molecular behavior of water on titanium dioxide nanotubes: a molecular dynamics simulation study. *J Chem Eng Data.* 2016;61:4131–4138.
- [237] Zhang Q, Chan K-Y, Quirke N. Molecular dynamics simulation of water confined in a nanopore of amorphous silica. *Mol Simul.* 2009;35:1215–1223.
- [238] Renou R, Szymczyk A, Ghoufi A. Influence of the pore length on the properties of water confined in a silica nanopore. *Mol Phys.* 2014;112:2275–2281.
- [239] Dickey AN, Stevens MJ. Site-dipole field and vortices in confined water. *Phys Rev E.* 2012;86:051601.
- [240] Ishikawa S, Sakuma H, Tsuchiya N. Self-diffusion of water molecules confined between quartz surfaces at elevated temperatures by molecular dynamics simulations. *J Mineral Petrol Sci.* 2016;111:297–302.
- [241] Patsahan T, Holovko M. Computer simulation study of the diffusion of water molecules confined in silica gel. *Condens Matter Phys.* 2004;7:3–13.
- [242] Siboulet B, Molina J, Coasne B, et al. Water self-diffusion at the surface of silica glasses: effect of hydrophilic to hydrophobic transition. *Mol Phys.* 2013;111:3410–3417.
- [243] Karzar Jeddi M, Romero-Vargas Castrillón S. Dynamics of water monolayers confined by chemically heterogeneous surfaces: observation of surface-induced anisotropic diffusion. *J Phys Chem B.* 2017;121:9666–9675.
- [244] Lerbret A, Lelong G, Mason PE, et al. Water confined in cylindrical pores: a molecular dynamics study. *Food Biophys.* 2011;6:233–240.
- [245] Qomi MJA, Bauchy M, Ulm FJ, et al. Anomalous composition-dependent dynamics of nanoconfined water in the interlayer of disordered calcium-silicates. *J Chem Phys.* 2014;140:054515.
- [246] Hou D, Lu C, Zhao T, et al. Structural, dynamic and mechanical evolution of water confined in the nanopores of disordered calcium silicate sheets. *Microfluid Nanofluidics.* 2015;19:1309–1323.
- [247] Hou D, Li Z, Zhao T, et al. Water transport in the nano-pore of the calcium silicate phase: reactivity, structure and dynamics. *Phys Chem Chem Phys.* 2015;17:1411–1423.
- [248] Hou D, Li D, Zhao T, et al. Confined water dissociation in disordered silicate nanometer-channels at elevated temperatures: mechanism, dynamics and impact on substrates. *Langmuir.* 2016;32:4153–4168.
- [249] Li D, Zhao W, Hou D, et al. Molecular dynamics study on the chemical bound, physical adsorbed and ultra-confined water molecules in the nano-pore of calcium silicate hydrate. *Constr Build Mater.* 2017;151:563–574.
- [250] Boek ES. Molecular dynamics simulations of interlayer structure and mobility in hydrated Li-, Na- and K-montmorillonite clays. *Mol Phys.* 2014;112:1472–1483.
- [251] Boğan A, Rotenberg B, Marry V, et al. Hydrodynamics in clay nanopores. *J Phys Chem C.* 2011;115:16109–16115.
- [252] Rao Q, Xiang Y, Leng Y. Molecular simulations on the structure and dynamics of water-methane fluids between Na-montmorillonite clay surfaces at elevated temperature and pressure. *J Phys Chem C.* 2013;117:14061–14069.
- [253] Zhou J, Lu X, Boek ES. Confined water in tunnel nanopores of sepiolite: insights from molecular simulations. *Am Mineral.* 2016;101:713–718.
- [254] Smirnov KS, Bougeard D. A molecular dynamics study of structure and short-time dynamics of water in kaolinite. *J Phys Chem B.* 1999;103:5266–5273.
- [255] Michot LJ, Ferrage E, Jiménez-Ruiz M, et al. Anisotropic features of water and ion dynamics in synthetic Na- and Ca-smectites with tetrahedral layer charge. A combined quasi-elastic neutron-scattering and molecular dynamics simulations study. *J Phys Chem C.* 2012;116:16619–16633.
- [256] Stanley HE, Kumar P, Franzese G, et al. Liquid polyamorphism: some unsolved puzzles of water in bulk, nanoconfined, and biological environments. *AIP Conf Proc.* 2008;982:251–271.
- [257] Segá M, Vallauri R, Melchionna S. Diffusion of water in confined geometry: the case of a multilamellar bilayer. *Phys Rev E.* 2005;72:041201.
- [258] McDonnell MT, Greeley DA, Kit KM, et al. Molecular dynamics simulations of hydration effects on solvation, diffusivity, and permeability in Chitosan/Chitin films. *J Phys Chem B.* 2016;120:8997–9010.
- [259] Hua L, Huang X, Zhou R, et al. Dynamics of water confined in the interdomain region of a multidomain protein. *J Phys Chem B.* 2006;110:3704–3711.
- [260] Berrod Q, Hanot S, Guillermo A, et al. Water sub-diffusion in membranes for fuel cells. *Sci Rep.* 2017;7:8326.
- [261] Gavazzoni C, Giovambattista N, Netz PA, et al. Structure and mobility of water confined in AlPO₄-54 nanotubes. *J Chem Phys.* 2017;146:234509.
- [262] Ding M, Szymczyk A, Goujon F, et al. Structure and dynamics of water confined in a polyamide reverse-osmosis membrane: a molecular-simulation study. *J Membrane Sci.* 2014;458:236–244.

- [263] Won CY, Aluru NR. Structure and dynamics of water confined in a boron nitride nanotube. *J Phys Chem B*. 2008;112:1812–1818.
- [264] Di Napoli S, Gamba Z. Structural and dynamical properties of water confined between two hydrophilic surfaces. *Phys B*. 2009;404:2883–2886.
- [265] Beckstein O, Sansom MSP. Liquid-vapor oscillations of water in hydrophobic nanopores. *Proc Natl Acad Sci USA*. 2003;100:7063–7068.
- [266] Brovchenko I, Geiger A, Oleinikova A, et al. Phase coexistence and dynamic properties of water in nanopores. *Eur Phys J E*. 2003;12:69–76.
- [267] Cui ST. Molecular self-diffusion in nanoscale cylindrical pores and classical Fick's law predictions. *J Chem Phys*. 2005;123:4–7.
- [268] Yamashita K, Daiguji H. Coarse-grained molecular dynamics simulations of capillary evaporation of water confined in hydrophilic mesopores. *Mol Phys*. 2016;114:884–894.
- [269] Köhler MH, Bordin JR, da Silva LB, et al. Breakdown of the Stokes–Einstein water transport through narrow hydrophobic nanotubes. *Phys Chem Chem Phys*. 2017;19:12921–12927.
- [270] Kumar P, Buldyrev SV, Starr FW, et al. Thermodynamics, structure, and dynamics of water confined between hydrophobic plates. *Phys Rev E – Stat Nonlinear, Soft Matter Phys*. 2005;72:1–12.
- [271] Kumar P, Han S, Stanley HE. Anomalies of water and hydrogen bond dynamics in hydrophobic nanoconfinement. *J Phys Condens Matter*. 2009;21:504108.
- [272] Bai J, Zeng XC. Polymorphism and polyamorphism in bilayer water confined to slit nanopore under high pressure. *Proc Natl Acad Sci USA*. 2012;109:21240–21245.
- [273] Choudhury N. Effect of surface hydrophobicity on the dynamics of water at the nanoscale confinement: a molecular dynamics simulation study. *Chem Phys*. 2013;421:68–76.
- [274] Bauer BA, Ou S, Patel S, et al. Dynamics and energetics of hydrophobically confined water. *Phys Rev E*. 2012;85:051506.
- [275] Han S, Choi MY, Kumar P, et al. Phase transitions in confined water nanofilms. *Nat Phys*. 2010;6:685–689.
- [276] Marañón Di Leo J, Marañón J. Confined water in nanotube. *J Mol Struct THEOCHEM*. 2003;623:159–166.
- [277] Han KN, Bernardi S, Wang L, et al. Water structure and transport in zeolites with pores in one or three dimensions from molecular dynamics simulations. *J Phys Chem C*. 2017;121:381–391.
- [278] Shirono K, Daiguji H. Dipole moments of water molecules confined in Na-LSX zeolites – molecular dynamics simulations including polarization of water. *Chem Phys Lett*. 2006;417:251–255.
- [279] Ju SP, Chang JG, Sen LJ, et al. The effects of confinement on the behavior of water molecules between parallel Au plates of (001) planes. *J Chem Phys*. 2005;122:1–5.
- [280] Lane JMD, Chandross M, Stevens MJ, et al. Water in nanoconfinement between hydrophilic self-assembled monolayers. *Langmuir*. 2008;24:5209–5212.
- [281] Franco LFM, Castier M, Economou IG. Diffusion in homogeneous and in inhomogeneous media: a new unified approach. *J Chem Theory Comput*. 2016;12:5247–5255.
- [282] Franco LFM, Castier M, Economou IG. Anisotropic parallel self-diffusion coefficients near the calcite surface: a molecular dynamics study. *J Chem Phys*. 2016;145:084702.
- [283] Mittal J, Truskett TM, Errington JR, et al. Layering and position-dependent diffusive dynamics of confined fluids. *Phys Rev Lett*. 2008;100:145901.
- [284] Von Hansen Y, Gekle S, Netz RR. Anomalous anisotropic diffusion dynamics of hydration water at lipid membranes. *Phys Rev Lett*. 2013;111:118103.
- [285] Carmer J, Van Swol F, Truskett TM. Note: position-dependent and pair diffusivity profiles from steady-state solutions of color reaction-counterdiffusion problems. *J Chem Phys*. 2014;141:046101.
- [286] Simonnin P, Noettinger B, Nieto-Draghi C, et al. Diffusion under confinement: hydrodynamic finite-size effects in simulation. *J Chem Theory Comput*. 2017;13:2881–2889.
- [287] Mills R. Self-diffusion in normal and heavy water in the range 1–45°. *J Phys Chem*. 1973;77:685–688.
- [288] Jonas J, DeFries T, Wilbur DJ. Molecular motions in compressed liquid water. *J Chem Phys*. 1976;65:582–588.
- [289] Krynicki K, Green CD, Sawyer DW. Pressure and temperature dependence of self-diffusion in water. *Faraday Discuss Chem Soc*. 1978;66:199–208.
- [290] Lamb WJ, Hoffman GA, Jonas J. Self-diffusion in compressed supercritical water. *J Chem Phys*. 1981;74:6875–6880.
- [291] Prielmeier FX, Lang EW, Speedy RJ, et al. Diffusion in supercooled water to 300MPa. *Phys Rev Lett*. 1987;59:1128–1131.
- [292] Prielmeier FX, Lang EW, Speedy RJ, et al. The pressure dependence of self-diffusion in supercooled light and heavy water. *Ber Bunsenges Phys Chem*. 1988;92:1111–1117.
- [293] Cunsolo A, Orecchini A, Petrillo C, et al. Quasielastic neutron scattering investigation of the pressure dependence of molecular motions in liquid water. *J Chem Phys*. 2006;124:084503.
- [294] Yoshida K, Matubayasi N, Nakahara M. Self-diffusion coefficients for water and organic solvents at high temperatures along the coexistence curve. *J Chem Phys*. 2008;129:214501.
- [295] Klotz S, Strassle T, Bove LE. Quasi-elastic neutron scattering in the multi-GPa range and its application to liquid water. *Appl Phys Lett*. 2013;103:193504.
- [296] Bove LE, Klotz S, Strässle T, et al. Translational and rotational diffusion in water in the gigapascal range. *Phys Rev Lett*. 2013;111:185901.
- [297] Suárez-Iglesias O, Medina I, de los Ángeles Sanz M, et al. Self-diffusion in molecular fluids and noble gases: available data. *J Chem Eng Data*. 2015;60:2757–2817.
- [298] Engkvist O, Åstrand PO, Karlström G. Accurate intermolecular potentials obtained from molecular wave functions: bridging the gap between quantum chemistry and molecular simulations. *Chem Rev*. 2000;100:4087–4108.
- [299] Laasonen K, Sprik M, Parrinello M, et al. “*Ab initio*” liquid water. *J Chem Phys*. 1993;99:9080–9089.
- [300] Sprik M, Hutter J, Parrinello M. *Ab initio* molecular dynamics simulation of liquid water: comparison of three gradient-corrected density functionals. *J Chem Phys*. 1996;105:1142–1152.
- [301] Silvestrelli PL, Parrinello M. Structural, electronic, and bonding properties of liquid water from first principles. *J Chem Phys*. 1999;111:3572–3580.
- [302] Izvekov S, Voth GA. Car-Parrinello molecular dynamics simulation of liquid water: new results. *J Chem Phys*. 2002;116:10372–10376.
- [303] Izvekov S, Parrinello M, Burnham CJ, et al. Effective force fields for condensed phase systems from *ab initio* molecular dynamics simulation: a new method for force-matching. *J Chem Phys*. 2004;120:10896–10913.
- [304] Allesch M, Schwegler E, Gygi F, et al. A first principles simulation of rigid water. *J Chem Phys*. 2004;120:5192–5198.
- [305] Krallafa A, Adda A, Seddiki A, et al. Molecular dynamics simulation of water in the low temperature region. *AIP Conf Proc*. 2012;1456:215–222.
- [306] Jonchiere R, Seitsonen AP, Ferlat G, et al. Van der Waals effects in *ab initio* water at ambient and supercritical conditions. *J Chem Phys*. 2011;135:154503.
- [307] Xantheas SS. Interaction potentials for water from accurate cluster calculations. *Struct Bond*. 2005;116:119–148.
- [308] Jorgensen WL, Tirado-Rives J. Potential energy functions for atomic-level simulations of water and organic and biomolecular systems. *Proc Natl Acad Sci USA*. 2005;102:6665–6670.
- [309] Asthagiri D, Pratt LR, Kress JD. Free energy of liquid water on the basis of quasichemical theory and *ab initio* molecular dynamics. *Phys Rev E*. 2003;68:041505.
- [310] Grossman JC, Schwegler E, Draeger EW, et al. Towards an assessment of the accuracy of density functional theory for first principles simulations of water. *J Chem Phys*. 2004;120:300–311.
- [311] Schwegler E, Grossman JC, Gygi F, et al. Towards an assessment of the accuracy of density functional theory for first principles simulations of water. II. *J Chem Phys*. 2004;121:5400–5409.
- [312] Fernández-Serra MV, Artacho E. Network equilibration and first-principles liquid water. *J Chem Phys*. 2004;121:11136–11144.

- [313] Kuo IFW, Mundy CJ, McGrath MJ, et al. Liquid water from first principles: investigation of different sampling approaches. *J Phys Chem B*. 2004;108:12990–12998.
- [314] VandeVondele J, Mohamed F, Krack M, et al. The influence of temperature and density functional models in *ab initio* molecular dynamics simulation of liquid water. *J Chem Phys*. 2005;122:014515.
- [315] Sit PH-L, Marzari N. Static and dynamical properties of heavy water at ambient conditions from first-principles molecular dynamics. *J Chem Phys*. 2005;122:204510.
- [316] Fernández-Serra MV, Ferlat G, Artacho E. Two exchange-correlation functionals compared for first-principles liquid water. *Mol Simul*. 2005;31:361–366.
- [317] Todorova T, Seitsonen AP, Hutter J, et al. Molecular dynamics simulation of liquid water: hybrid density functionals. *J Phys Chem B*. 2006;110:3685–3691.
- [318] Lee H-S, Tuckerman ME. Structure of liquid water at ambient temperature from *ab initio* molecular dynamics performed in the complete basis set limit. *J Chem Phys*. 2006;125:154507.
- [319] Lee H-S, Tuckerman ME. Dynamical properties of liquid water from *ab initio* molecular dynamics performed in the complete basis set limit. *J Chem Phys*. 2007;126:164501.
- [320] Guidon M, Schiffmann F, Hutter J, et al. *Ab initio* molecular dynamics using hybrid density functionals. *J Chem Phys*. 2008;128:214104.
- [321] Yoo S, Zeng XC, Xantheas SS. On the phase diagram of water with density functional theory potentials: the melting temperature of ice Ih with the Perdew–Burke–Ernzerhof and Becke–Lee–Yang–Parr functionals. *J Chem Phys*. 2009;130:221102.
- [322] Kuhne TD, Krack M, Parrinello M. Static and dynamical properties of liquid water from first principles by a novel car-parrinello-like approach. *J Chem Theory Comput*. 2009;5:235–241.
- [323] Ma Z, Zhang Y, Tuckerman ME. *Ab initio* molecular dynamics study of water at constant pressure using converged basis sets and empirical dispersion corrections. *J Chem Phys*. 2012;137:044506.
- [324] Lin IC, Seitsonen AP, Tavernelli I, et al. Structure and dynamics of liquid water from *ab initio* molecular dynamics—comparison of BLYP, PBE, and revPBE density functionals with and without van der waals corrections. *J Chem Theory Comput*. 2012;8:3902–3910.
- [325] Distasio RA, Santra B, Li Z, et al. The individual and collective effects of exact exchange and dispersion interactions on the *ab initio* structure of liquid water. *J Chem Phys*. 2014;141:084502.
- [326] Bankura A, Karmakar A, Carnevale V, et al. Structure, dynamics, and spectral diffusion of water from first-principles molecular dynamics. *J Phys Chem C*. 2014;118:29401–29411.
- [327] Del Ben M, Hutter J, VandeVondele J. Probing the structural and dynamical properties of liquid water with models including non-local electron correlation. *J Chem Phys*. 2015;143:054506.
- [328] Ambrosio F, Miceli G, Pasquarello A. Structural, dynamical, and electronic properties of liquid water: a hybrid functional study. *J Phys Chem B*. 2016;120:7456–7470.
- [329] Galib M, Duignan TT, Misteli Y, et al. Mass density fluctuations in quantum and classical descriptions of liquid water. *J Chem Phys*. 2017;146:244501.
- [330] Chen M, Ko H, Remsing RC, et al. *Ab initio* theory and modeling of water. *Proc Natl Acad Sci USA*. 2017;114:10846–10851.
- [331] Karmakar A, Chandra A. Water under supercritical conditions: hydrogen bonds, polarity, and vibrational frequency fluctuations from *Ab initio* simulations with a dispersion corrected density functional. *ACS Omega*. 2018;3:3453–3462.
- [332] Dawson W, Gygi F. Equilibration and analysis of first-principles molecular dynamics simulations of water. *J Chem Phys*. 2018;148:124501.
- [333] Zheng L, Chen M, Sun Z, et al. Structural, electronic, and dynamical properties of liquid water by *ab initio* molecular dynamics based on SCAN functional within the canonical ensemble. *J Chem Phys*. 2018;148:164505.
- [334] Karmakar A, Chandra A. Dynamics of vibrational spectral diffusion in water: effects of dispersion interactions, temperature, density, system size and fictitious orbital mass. *J Mol Liq*. 2018;249:169–178.
- [335] Manzano H, Zhang W, Raju M, et al. Benchmark of ReaxFF force field for subcritical and supercritical water. *J Chem Phys*. 2018;148:234503.
- [336] van Duin ACT, Dasgupta S, Lorant F, et al. ReaxFF: a reactive force field for hydrocarbons. *J Phys Chem A*. 2001;105:9396–9409.
- [337] Fogarty JC, Aktulga HM, Grama AY, et al. A reactive molecular dynamics simulation of the silica-water interface. *J Chem Phys*. 2010;132:174704.
- [338] Pascal TA, Scharf D, Jung Y, et al. On the absolute thermodynamics of water from computer simulations: A comparison of first-principles molecular dynamics, reactive and empirical force fields. *J Chem Phys*. 2012;137:244507.
- [339] Rimsza JM, Yeon J, van Duin ACT, et al. Water interactions with nanoporous silica: comparison of ReaxFF and *ab initio* based molecular dynamics simulations. *J Phys Chem C*. 2016;120:24803–24816.
- [340] Zhang W, van Duin ACT. Second-generation ReaxFF water force field: improvements in the description of water density and OH-anion diffusion. *J Phys Chem B*. 2017;121:6021–6032.
- [341] Teleman O, Wallqvist A. Ewald summation retards translational motion in molecular dynamic simulations of water. *Int J Quantum Chem*. 1990;38:245–249.
- [342] Teleman O. An efficient way to conserve the total energy in molecular dynamics simulations; boundary effects on energy conservation and dynamic properties. *Mol Sim*. 1988;1:345–355.
- [343] Dünweg B, Kremer K. Molecular dynamics simulation of a polymer chain in solution. *J Chem Phys*. 1993;99:6983–6997.
- [344] Moultois OA, Zhang Y, Tsimpanogiannis IN, et al. System-size corrections for self-diffusion coefficients calculated from molecular dynamics simulations: the case of CO₂, *n*-alkanes, and poly(ethylene glycol) dimethyl ethers. *J Chem Phys*. 2016;145:074109.
- [345] Jamali SH, Wolff L, Becker TM, et al. Finite-size effects of binary mutual diffusion coefficients from molecular dynamics. *J Chem Theory Comput*. 2018;14:2667–2677.
- [346] Berendsen HJC, Postma JPM, van Gunsteren WF, et al. Interaction models for water in relation to protein hydration. In: Pullman B, editor. *Intermolecular forces*. Dordrecht: D. Reidel Publishing Company; 1981. p. 331–342.
- [347] Pranami G, Lamm MH. Estimating error in diffusion coefficients derived from molecular dynamics simulations. *J Chem Theory Comput*. 2015;11:4586–4592.
- [348] Wang B, Kuo J, Bae SC, et al. When Brownian diffusion is not Gaussian. *Nat Mater*. 2012;11:481–485.
- [349] Casalegno M, Raos G, Appetecchi GB, et al. From nanoscale to microscale: crossover in the diffusion dynamics within two pyrrolidinium-based ionic liquids. *J Phys Chem Lett*. 2017;8:5196–5202.
- [350] Lamoureux G, MacKerell AD, Roux B. A simple polarizable model of water based on classical Drude oscillators. *J Chem Phys*. 2003;119:5185–5197.
- [351] Habershon S, Markland TE, Manolopoulos DE. Competing quantum effects in the dynamics of a flexible water model. *J Chem Phys*. 2009;131:024501.
- [352] Ben-Naim A, Stillinger FH. Aspects of the statistical-mechanical theory of water. In: RA Horne, editor. *Structure and transport processes in water and aqueous solutions*. New York: Wiley-Interscience; 1972. p. 295–330.
- [353] Stillinger FH, Rahman A. Molecular dynamics study of temperature effects on water structure and kinetics. *J Chem Phys*. 1972;57:1281–1292.
- [354] Matsuoka O, Clementi E, Yoshimine M. CI study of the water dimer potential surface. *J Chem Phys*. 1976;64:1351–1361.
- [355] Jorgensen WL. Quantum and statistical mechanical studies of liquids. 10. transferable intermolecular potential functions for water, alcohols, and ethers. application to liquid water. *J Am Chem Soc*. 1981;103:335–340.
- [356] Dang LX, Pettitt BM. Simple intramolecular model potentials for water. *J Phys Chem*. 1987;91:3349–3354.
- [357] Mahoney MW, Jorgensen WL. A five-site model for liquid water and the reproduction of the density anomaly by rigid,

- nonpolarizable potential functions. *J Chem Phys.* 2000;112:8910–8922.
- [358] Guillot B. A reappraisal of what we have learnt during three decades of computer simulations on water. *J Mol Liq.* 2002;101:219–260.
- [359] Pieniazek PA, Tainter CJ, Skinner JL. Interpretation of the water surface vibrational sum-frequency spectrum. *J Chem Phys.* 2011;135:044701.
- [360] Jorgensen WL, Madura JD. Temperature and size dependence for monte carlo simulations of TIP4P water. *Mol Phys.* 1985;56:1381–1392.
- [361] Rick SW. A reoptimization of the five-site water potential (TIP5P) for use with Ewald sums. *J Chem Phys.* 2004;120:6085–6093.
- [362] Lopes PEM, Roux B, MacKerell AD. Molecular modeling and dynamics studies with explicit inclusion of electronic polarizability: theory and applications. *Theor Chem Acc.* 2009;124:11–28.
- [363] Schwörer M, Breitenfeld B, Tröster P, et al. Coupling density functional theory to polarizable force fields for efficient and accurate Hamiltonian molecular dynamics simulations. *J Chem Phys.* 2013;138:244103.
- [364] Qi R, Wang LP, Wang Q, et al. United polarizable multipole water model for molecular mechanics simulation. *J Chem Phys.* 2015;143:014504.
- [365] Yu H, Van Gunsteren WF. Charge-on-spring polarizable water models revisited: from water clusters to liquid water to ice. *J Chem Phys.* 2004;121:9549–9564.
- [366] Paricaud P, Předota M, Chialvo AA, et al. From dimer to condensed phases at extreme conditions: accurate predictions of the properties of water by a Gaussian charge polarizable model. *J Chem Phys.* 2005;122:244511.
- [367] Orozco GA, Moulton OA, Jiang H, et al. Molecular simulation of thermodynamic and transport properties for the H₂O + NaCl system. *J Chem Phys.* 2014;141:234507.
- [368] Jiang H, Mester Z, Moulton OA, et al. Thermodynamic and transport properties of H₂O + NaCl from polarizable force fields. *J Chem Theory Comput.* 2015;11:3802–3810.
- [369] Jiang W, Hardy D, Phillips J, et al. High-performance scalable molecular dynamics simulations of a polarizable force field based on classical Drude oscillators in NAMD. *J Phys Chem Lett.* 2011;2:87–92.
- [370] Phillips JC, Braun R, Wang W, et al. Scalable molecular dynamics with NAMD. *J Comput Chem.* 2005;26:1781–1802.
- [371] Tironi IG, Brunne RM, Van Gunsteren WF. On the relative merits of flexible versus rigid models for use in computer simulations of molecular liquids. *Chem Phys Lett.* 1996;250:19–24.
- [372] Lemberg HL, Stillinger FH. Central-force model for liquid water. *J Chem Phys.* 1975;62:1677–1690.
- [373] Bopp P, Jansco G, Heinzinger K. An improved potential for non-rigid water molecules in the liquid phase. *Chem Phys Lett.* 1983;98:129–133.
- [374] Reimers JR, Watts RO, Klein ML. Intermolecular potential functions and the properties of water. *Chem Phys.* 1982;64:95–114.
- [375] Martí J, Guàrdia E, Padró JA. Dielectric properties and infrared spectra of liquid water: influence of the dynamic cross correlations. *J Chem Phys.* 1994;101:10883–10891.
- [376] Martí J, Padró JA, Guàrdia E. Molecular dynamics simulation of liquid water along the coexistence curve: hydrogen bonds and vibrational spectra. *J Chem Phys.* 1996;105:639–649.
- [377] Toukan K, Rahman A. Molecular-dynamics study of atomic motions in water. *Phys Rev B.* 1985;31:2643–2648.
- [378] Hess B, Saint-Martin H, Berendsen HJC. Flexible constraints: an adiabatic treatment of quantum degrees of freedom, with application to the flexible and polarizable mobile charge densities in harmonic oscillators model for water. *J Chem Phys.* 2002;116:9602–9610.
- [379] Saint-Martin H, Hernández-Cobos J, Bernal-Uruchurtu MI, et al. A mobile charge densities in harmonic oscillators (MCDHO) molecular model for numerical simulations: the water–water interaction. *J Chem Phys.* 2000;113:10899–10912.
- [380] Niesar U, Corongiu G, Clementi E, et al. Molecular dynamics simulations of liquid water using the NCC *ab initio* potential. *J Phys Chem.* 1990;94:7949–7956.
- [381] Babin V, Leforestier C, Paesani F. Development of a “first principles” water potential with flexible monomers: dimer potential energy surface, VRT spectrum, and second virial coefficient. *J Chem Theory Comput.* 2013;9:5395–5403.
- [382] Babin V, Medders GR, Paesani F. Development of a “first principles” water potential with flexible monomers. II: trimer potential energy surface, third virial coefficient, and small clusters. *J Chem Theory Comput.* 2014;10:1599–1607.
- [383] Speedy RJ, Angell CA. Isothermal compressibility of supercooled water and evidence for a thermodynamic singularity at -45°C. *J Chem Phys.* 1976;65:851–858.
- [384] Price WS, Ide H, Arata Y. Self-diffusion of supercooled water to 238K using PGSE NMR diffusion measurements. *J Phys Chem A.* 1999;103:448–450.
- [385] Holz M, Heil SR, Sacco A. Temperature-dependent self-diffusion coefficients of water and six selected molecular liquids for calibration in accurate 1H NMR PFG measurements. *Phys Chem Chem Phys.* 2000;2:4740–4742.
- [386] Huang Y-L, Merker T, Heilig M, et al. Molecular modeling and simulation of vapor-liquid equilibria of ethylene oxide, ethylene glycol, and water as well as their binary mixtures. *Ind Eng Chem Res.* 2012;51:7428–7440.
- [387] Mishima O, Stanley HE. The relationship between liquid, supercooled and glassy water. *Nature.* 1998;396:329–335.
- [388] Xu L, Mallamace F, Yan Z, et al. Appearance of a fractional Stokes–Einstein relation in water and a structural interpretation of its onset. *Nat Phys.* 2009;5:565–569.
- [389] Angell CA, Ito K, Moynihan CT. Thermodynamic determination of fragility in liquids and a fragile-to-strong liquid transition in water. *Nature.* 1999;398:492–495.
- [390] Mallamace F, Corsaro C, Stanley HE. A singular thermodynamically consistent temperature at the origin of the anomalous behavior of liquid water. *Sci Rep.* 2012;2:993.
- [391] Scala A, Starr FW, La Nave E, et al. Configurational entropy and diffusivity of supercooled water. *Nature.* 2000;406:166–169.
- [392] Rosenfeld Y. A quasi-universal scaling law for atomic transport in simple fluids. *J Phys: Condens Matter.* 1999;11:5415–5427.
- [393] Errington JR, Truskett TM, Mittal J. Excess-entropy-based anomalies for a waterlike fluid. *J Chem Phys.* 2006;125:244502.
- [394] Agarwal M, Singh M, Sharma R, et al. Relationship between structure, entropy, and diffusivity in water and water-like liquids. *J Phys Chem B.* 2010;114:6995–7001.
- [395] Chopra R, Truskett TM, Errington JR. On the use of excess entropy scaling to describe the dynamic properties of water. *J Phys Chem B.* 2010;114:10558–10566.
- [396] Yan Z, Buldyrev SV, Stanley HE. Relation of water anomalies to the excess entropy. *Phys Rev E.* 2008;78:051201.